Radiative Corrections in SIDIS from CLAS

Nathan Harrison[1,2]

[1]University of Connecticut
[2]Jefferson Lab

Precision Radiative Corrections for Next Generation Experiments
May 17, 2016

Outline

- Physics
  - motivation
  - SIDIS
  - TMDs & FFs
- Experiment
  - CEBAF at Jefferson National Lab
  - CLAS detector
  - E1-f data set
- Analysis
  - event selection and binning for $ep \rightarrow e\pi^{\pm}X$
  - acceptance studies (Monte Carlo)
  - radiative corrections
- Results
- Summary & conclusions

Physics Motivation

- Deep inelastic scattering (DIS) experiments at SLAC, HERA, and CERN during the 1970s, 80s, and 90s measured parton distribution functions (PDFs) that describe the behavior of quarks and gluons inside of nucleons.
- These PDFs depend on the longitudinal parton momentum fraction, x, and on the square of the momentum transferred between the scattered electron and the struck parton, Q^2, but are integrated over transverse momentum.
- Semi-inclusive DIS (SIDIS) gives access to transverse momentum dependent PDFs (TMDs).
- Studying TMDs may give insights into the quark orbital angular momentum contribution to the proton spin.

SIDIS kinematics

Goal: Study the transverse motion of quarks inside of the proton via semi-inclusive deep inelastic scattering (SIDIS):

$$l\,(k) + N\,(P) \to l'\,(k') + h\,(P_h) + X\,(P_X)$$

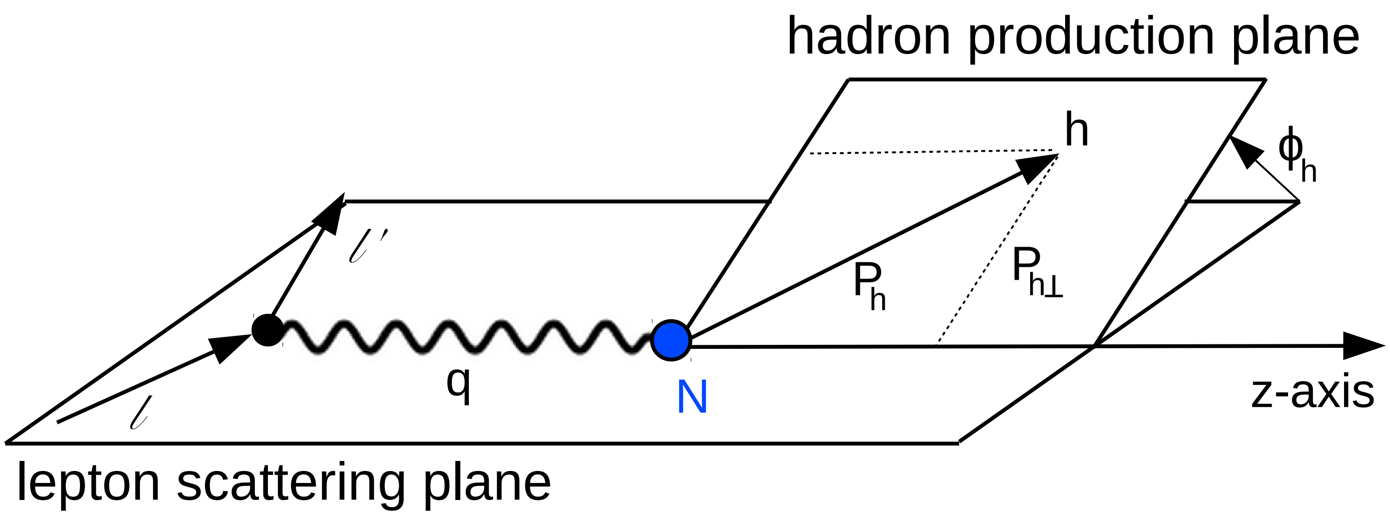

$$Q^2 = -q^2 = -\left(k - k'\right)^2, \qquad x = \frac{Q^2}{2P \cdot q}, \qquad y = \frac{P \cdot q}{P \cdot k}, \qquad \gamma = \frac{2Mx}{Q}$$

$$W^2 = \left(P + q\right)^2, \qquad z = \frac{P \cdot P_h}{P \cdot q}, \qquad \varepsilon = \frac{1 - y - \frac{1}{4}\gamma^2 y^2}{1 - y + \frac{1}{2}y^2 + \frac{1}{4}\gamma^2 y^2}$$

SIDIS cross-section

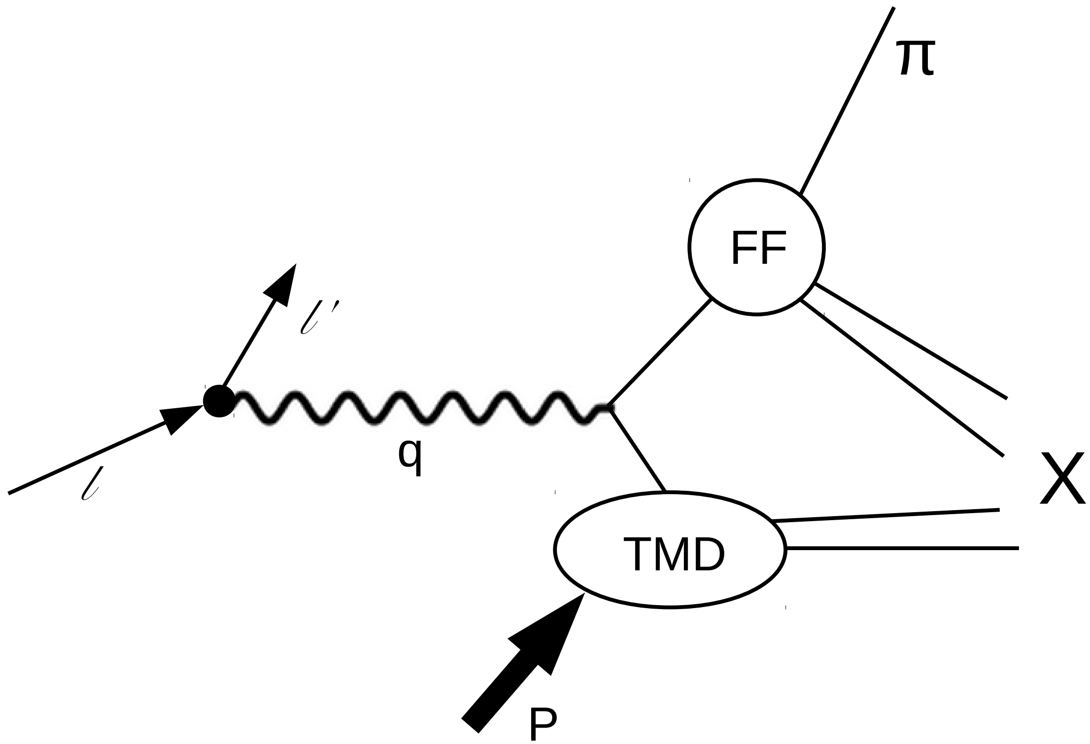

- Motion of quarks inside of the proton is described by TMDs.

- The process of the struck quark forming into a hadron ("hadronization") is described by fragmentation functions (FFs).

Assuming single photon exchange, the leptoproduction cross-section can be written as:

$$\frac{d^6\sigma}{dx\ dQ^2\ d\psi\ dz\ d\phi_h\ dP_{h\perp}^2} = \frac{1}{2E_b M x}\frac{\alpha^2 y}{8zQ^4} 2MW^{\mu\nu}L_{\mu\nu}$$

$L_{\mu\nu}$ is the leptonic tensor.

$W^{\mu\nu}$ is the hadronic tensor.

SIDIS cross-section

Expanding the contraction and integrating over ψ and the beam polarization, the cross-section for an unpolarized target can be written as

$$\frac{d^5\sigma}{dx\ dQ^2\ dz\ d\phi_h\ dP_{h\perp}^2} =$$

$$\underbrace{\frac{2\pi\alpha^2}{xyQ^2}\frac{y^2}{2(1-\epsilon)}\left(1+\frac{\gamma^2}{2x}\right)(F_{UU,T}+\epsilon F_{UU,L})}_{A_0}\left\{1+\underbrace{\frac{\sqrt{2\epsilon(1+\epsilon)}F_{UU}^{\cos\phi_h}}{(F_{UU,T}+\epsilon F_{UU,L})}}_{A_{UU}^{\cos\phi_h}}\cos\phi_h+\underbrace{\frac{\epsilon F_{UU}^{\cos 2\phi_h}}{(F_{UU,T}+\epsilon F_{UU,L})}}_{A_{UU}^{\cos 2\phi_h}}\cos 2\phi_h\right\}$$

According the the factorization theorem, structure functions can, in the Bjorken limit, be written as convolutions of TMDs and FFs:

$$F = \sum \mathrm{TMD} \otimes \mathrm{FF}$$

Bjorken Limit:

$$Q^2 \to \infty$$

$$2P\cdot q \to \infty$$

$$P\cdot P_h \to \infty$$

$$\text{fixed}\begin{cases} x = Q^2/2P\cdot q \\ z = P\cdot P_h/P\cdot q \end{cases}$$

The Boer-Mulders TMD

The Boer-Mulders function describes transversely polarized quarks inside of unpolarized nucleons; it is a quark distribution that quantifies a spin-orbit correlation.

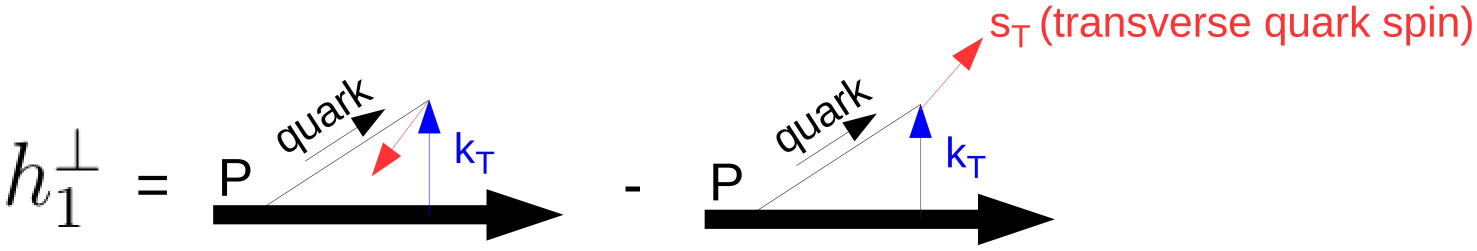

This difference of probabilities reflects the presence of a handedness inside the proton (P • (k_T x s_T)). If non-zero, there is a net transverse quark polarization.

Structure Functions, TMDs, and FFs

$$F_{UU,T} = \mathcal{C}\left[f_1 D_1\right],$$

$$F_{UU,L} = 0,$$

$$F_{UU}^{\cos\phi_h} = \frac{2M}{Q}\mathcal{C}\left[-\frac{\hat{\mathbf{h}}\cdot\mathbf{p}_T}{M_h}\left(xhH_1^\perp + \frac{M_h}{M}f_1\frac{\tilde{D}^\perp}{z}\right) - \frac{\hat{\mathbf{h}}\cdot\mathbf{k}_T}{M}\left(xf^\perp D_1 + \frac{M_h}{M}h_1^\perp\frac{\tilde{H}}{z}\right)\right]$$

$$F_{UU}^{\cos 2\phi_h} = \mathcal{C}\left[-\frac{2(\hat{\mathbf{h}}\cdot\mathbf{p}_T)(\hat{\mathbf{h}}\cdot\mathbf{k}_T) - \mathbf{p}_T\cdot\mathbf{k}_T}{MM_h}h_1^\perp H_1^\perp\right].$$

where $\hat{\mathbf{h}} = \mathbf{P}_{h\perp}/\left|\mathbf{P}_{h\perp}\right|$ and

$$\mathcal{C}\left[wfD\right] = x\sum_a e_a^2\int d^2\mathbf{k}_T\, d^2\mathbf{p}_T\,\delta^{(2)}(\mathbf{k}_T - \mathbf{p}_T - \mathbf{P}_{h\perp}/z)w(\mathbf{k}_T,\mathbf{p}_T)f^a(x,k_T^2)D^a(z,p_T^2)$$

- $A_{UU}^{\cos 2\phi_h}$ is sensitive to the Boer-Mulders effect at the twist-2 level while $A_{UU}^{\cos\phi_h}$ only has higher twist contributions.

- There is a flavor independent kinematic effect, known as the Cahn effect, to which $A_{UU}^{\cos\phi_h}$ is sensitive at the twist-3 level and to which $A_{UU}^{\cos 2\phi_h}$ is sensitive at the twist-4 level.

- By measuring both moments for both charged pion channels, it may be possible to isolate the flavor dependent Boer-Mulders effect from higher twist contributions such as the (mostly) flavor independent Cahn effect.

The Experiment

- CEBAF at Jefferson Lab

- The CLAS detector

- E1-f data set

CLAS

The Continuous Electron Beam Accelerator Facility's Large Acceptance Spectrometer

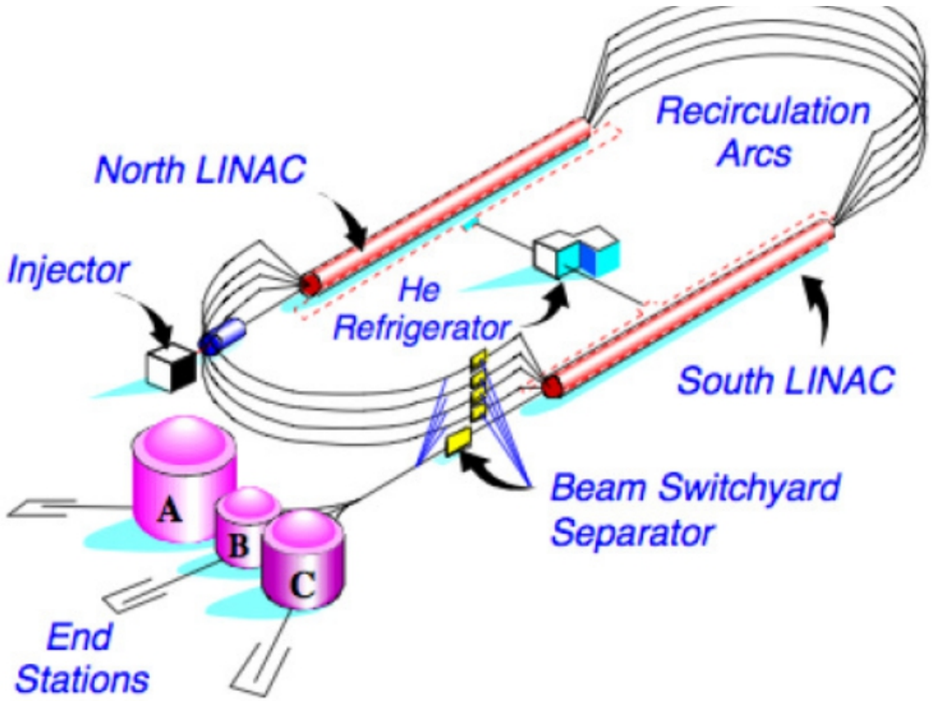

- Two 0.4 GeV linear accelerators.
- Nine recirculation arcs for five loops around the track.
- Continuous, polarized electron beam up to 6 GeV delivered simultaneously to 3 experimental halls.
- High luminosity of 0.5 x 10^{34} $(cm^2\ s)^{-1}$

- E1-f run: 5.498 GeV electron beam with ~75% polarization (averaged over for this analysis); unpolarized liquid hydrogen target; about 2 billion events; broad and comparable kinematic range for two channels:

$$ep \to e\pi^{\pm}X$$

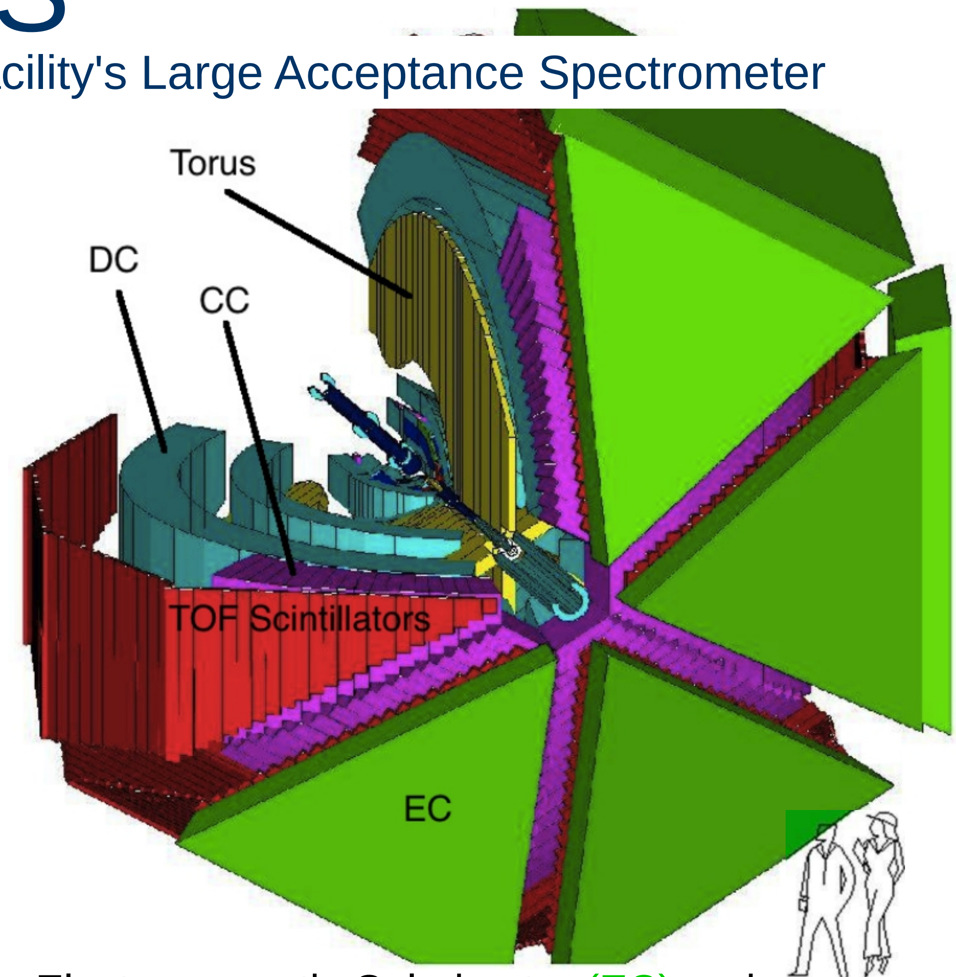

- Electromagnetic Calorimeter (EC) and Čerenkov Counter (CC) used in electron identification.

- Drift Chamber (DC) (3 regions) and time of flight Scintillators (SC) record position and timing information for each charged track.

- Torus magnet creates toroidal magnetic field which causes charged tracks to curve while preserving the φ_{lab} angle.

Analysis

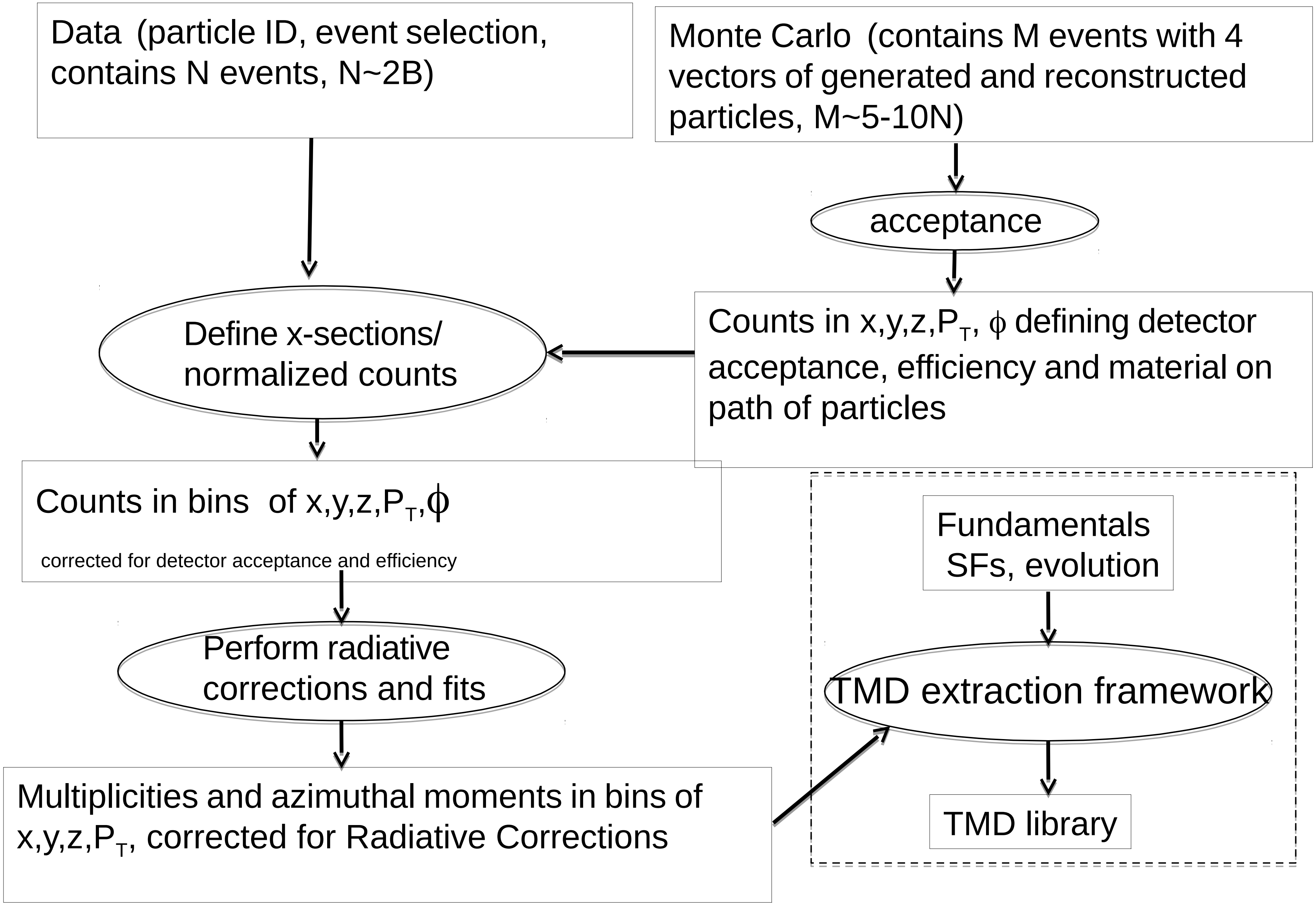
Data (particle ID, event selection, contains N events, N~2B)
Monte Carlo (contains M events with 4 vectors of generated and reconstructed particles, M~5-10N)
acceptance
Define x-sections/ normalized counts
Counts in x,y,z,P_T, ϕ defining detector acceptance, efficiency and material on path of particles
Counts in bins of x,y,z,P_T,ϕ
corrected for detector acceptance and efficiency
Perform radiative corrections and fits
Multiplicities and azimuthal moments in bins of x,y,z,P_T, corrected for Radiative Corrections
Fundamentals SFs, evolution
TMD extraction framework
TMD library

pion identification

(sector 1)

β vs momentum for positive tracks

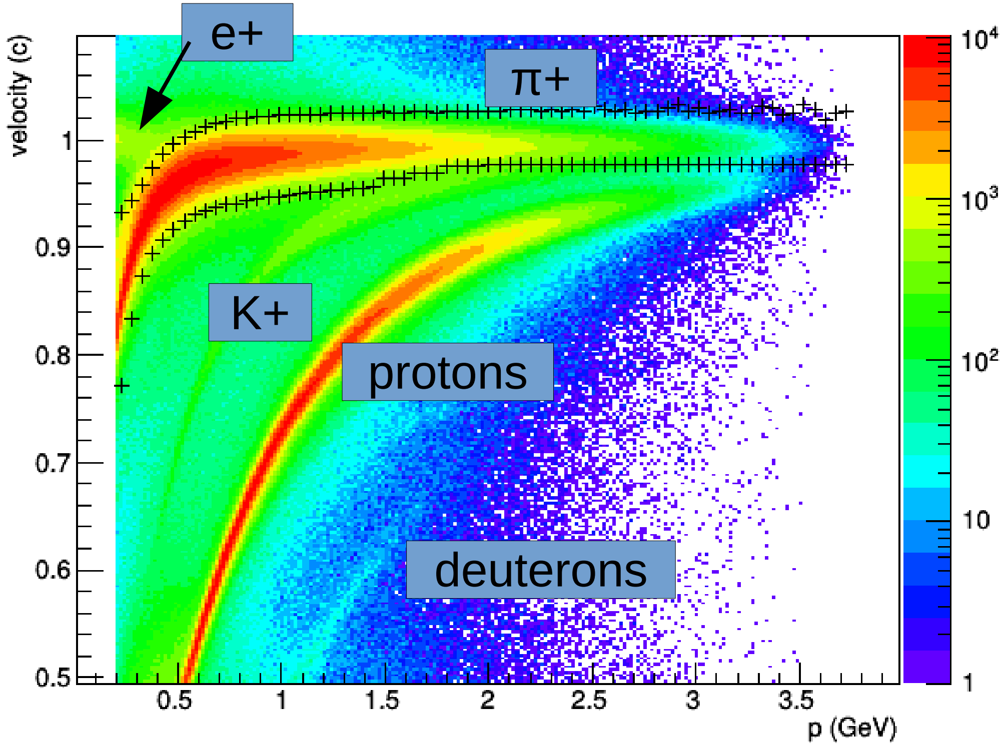

β vs momentum for negative tracks

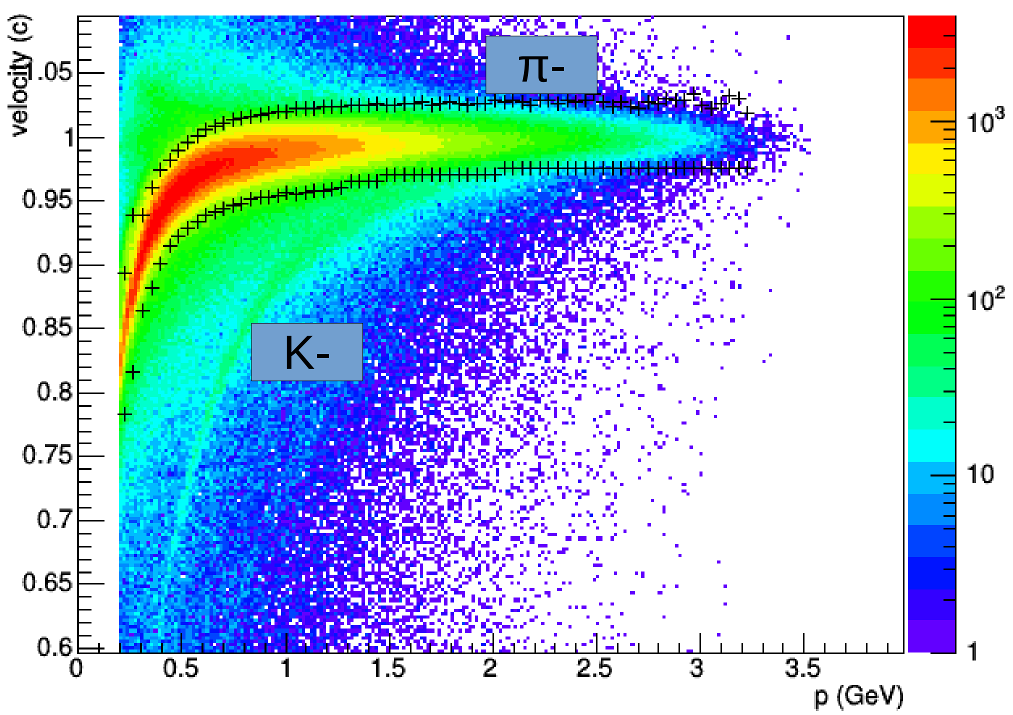

- 70 vertical slices fit with a gaussian

- 3σ cut at low momenta

- Cut tapers in at high momenta

SIDIS Cuts and Binning

π+ channel

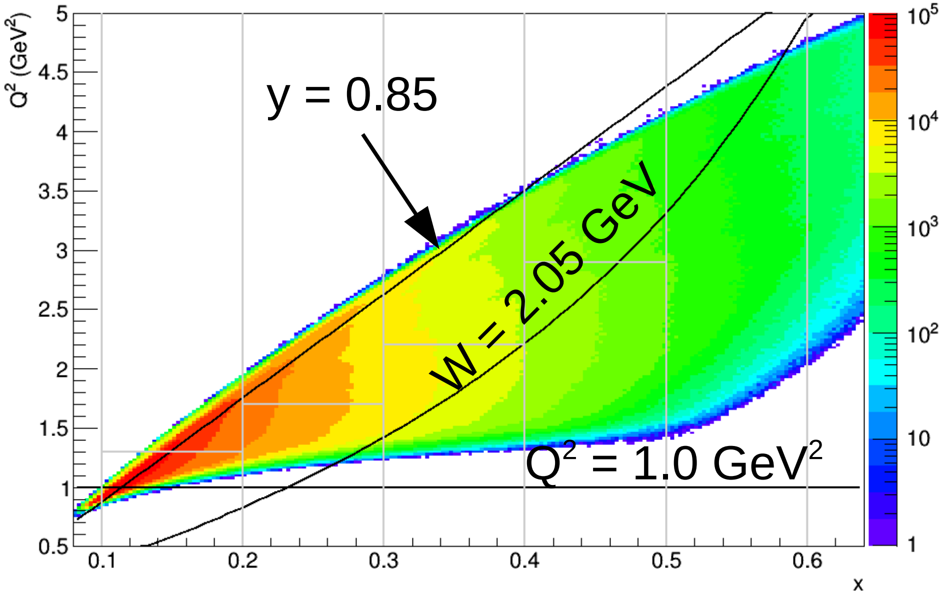

π- channel

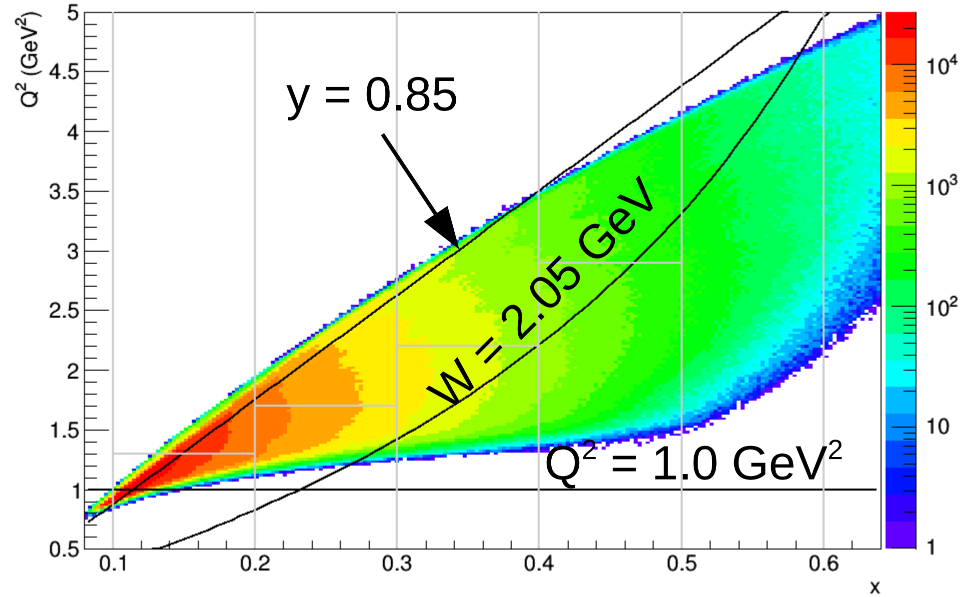

The DIS region is defined as $Q^2 > 1.0$ GeV^2 and $W > 2.05$ GeV.

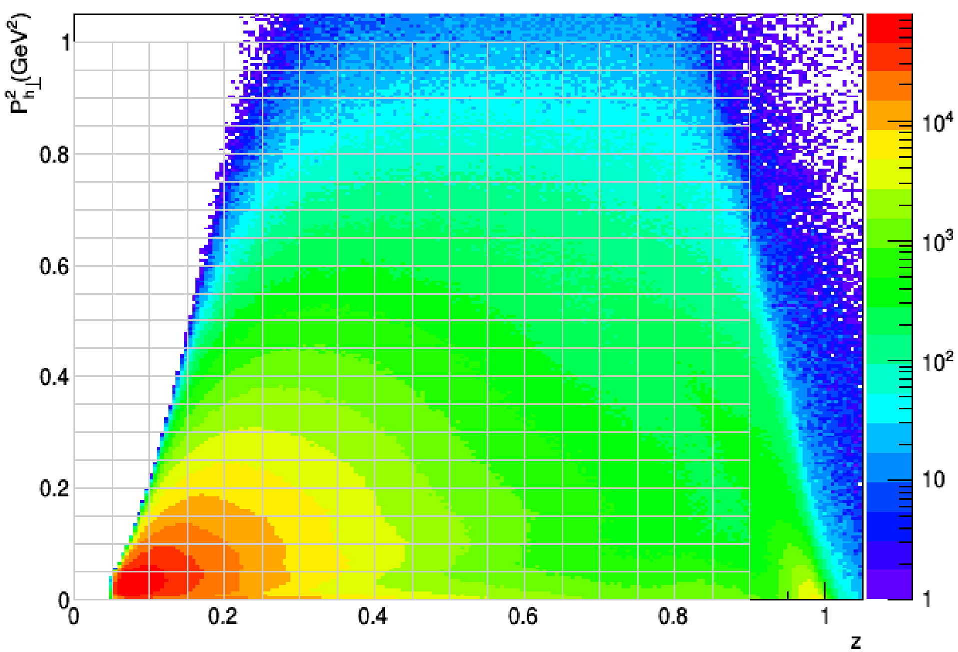

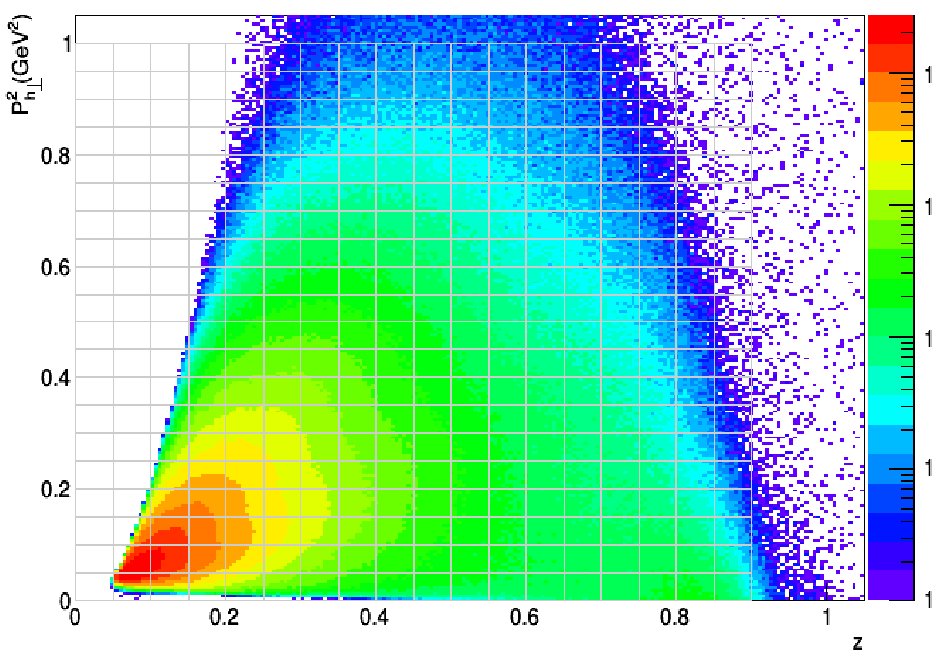

Simulation

- 1B SIDIS events are generated with a PYTHIA based event generator.

- 3 different models were used to study model dependence.

- Generated events are put into a GEANT based Monte Carlo simulation of the CLAS detector (GSim).

- Smearing and inefficiencies are introduced to the simulation to make it more realistic.

- The simulated data is then "cooked", processed, and analyzed in the same way as the E1-f data set.

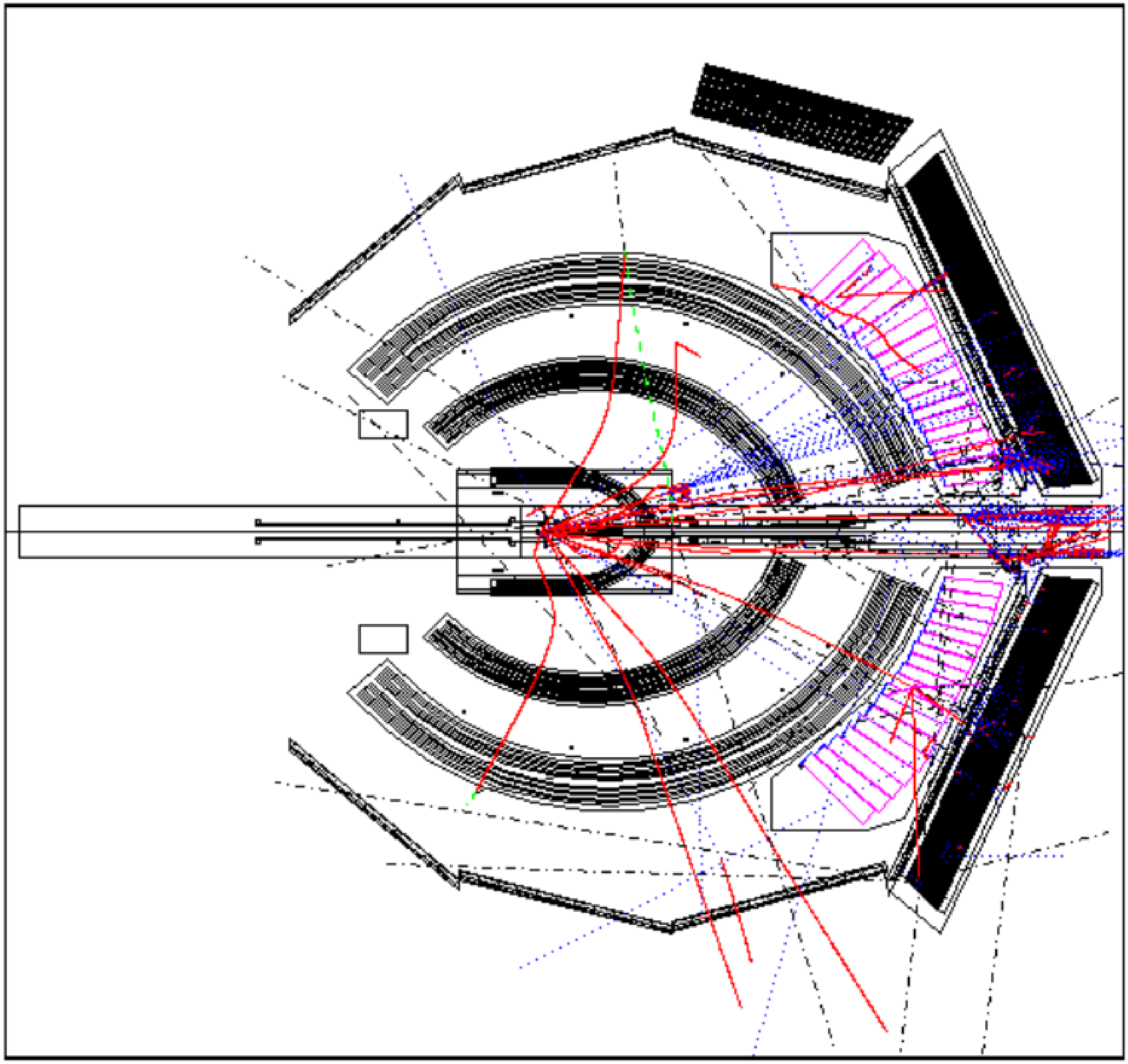

Above: Five generated events being reconstructed by GSim. Charged tracks are shown in red, neutral tracks in gray.

Monte Carlo φ generated, reconstructed, and acceptance for π+ (lowest x-Q^2 bin)

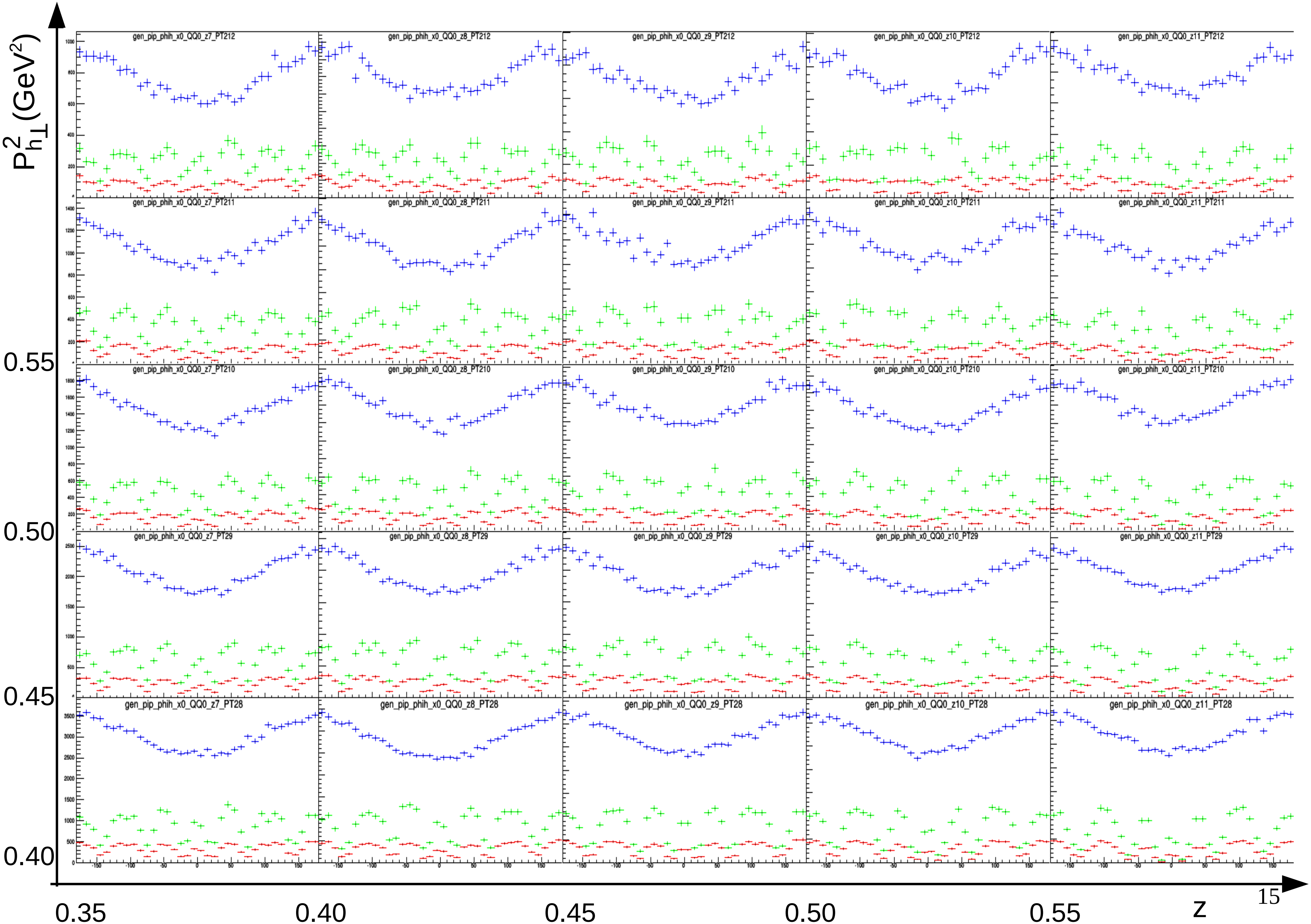

Monte Carlo φ generated, reconstructed, and acceptance for π+ (lowest x-Q^2 bin)

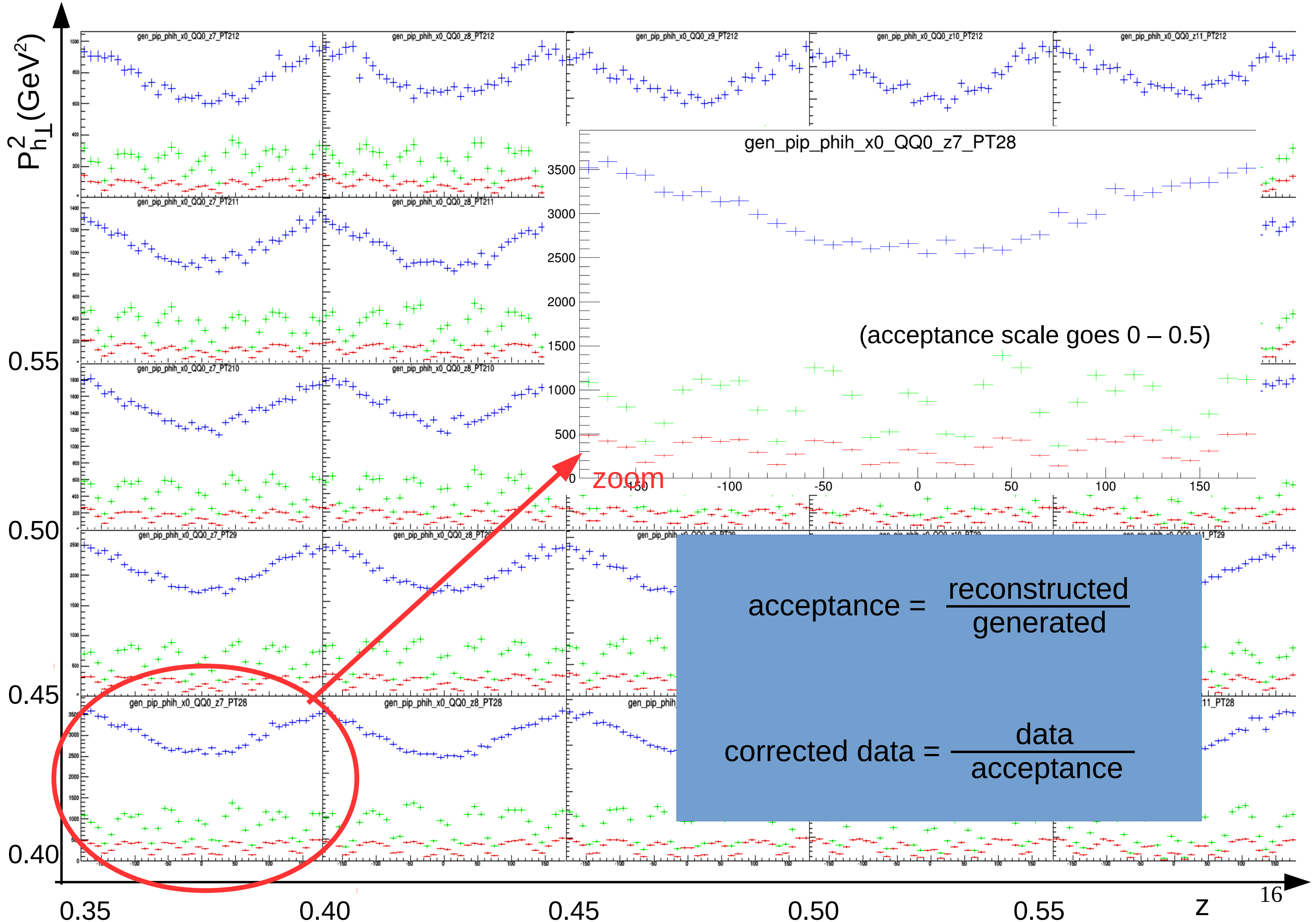

$$\text{acceptance} = \frac{\text{reconstructed}}{\text{generated}}$$

$$\text{corrected data} = \frac{\text{data}}{\text{acceptance}}$$

5-dimensional Acceptance Structure

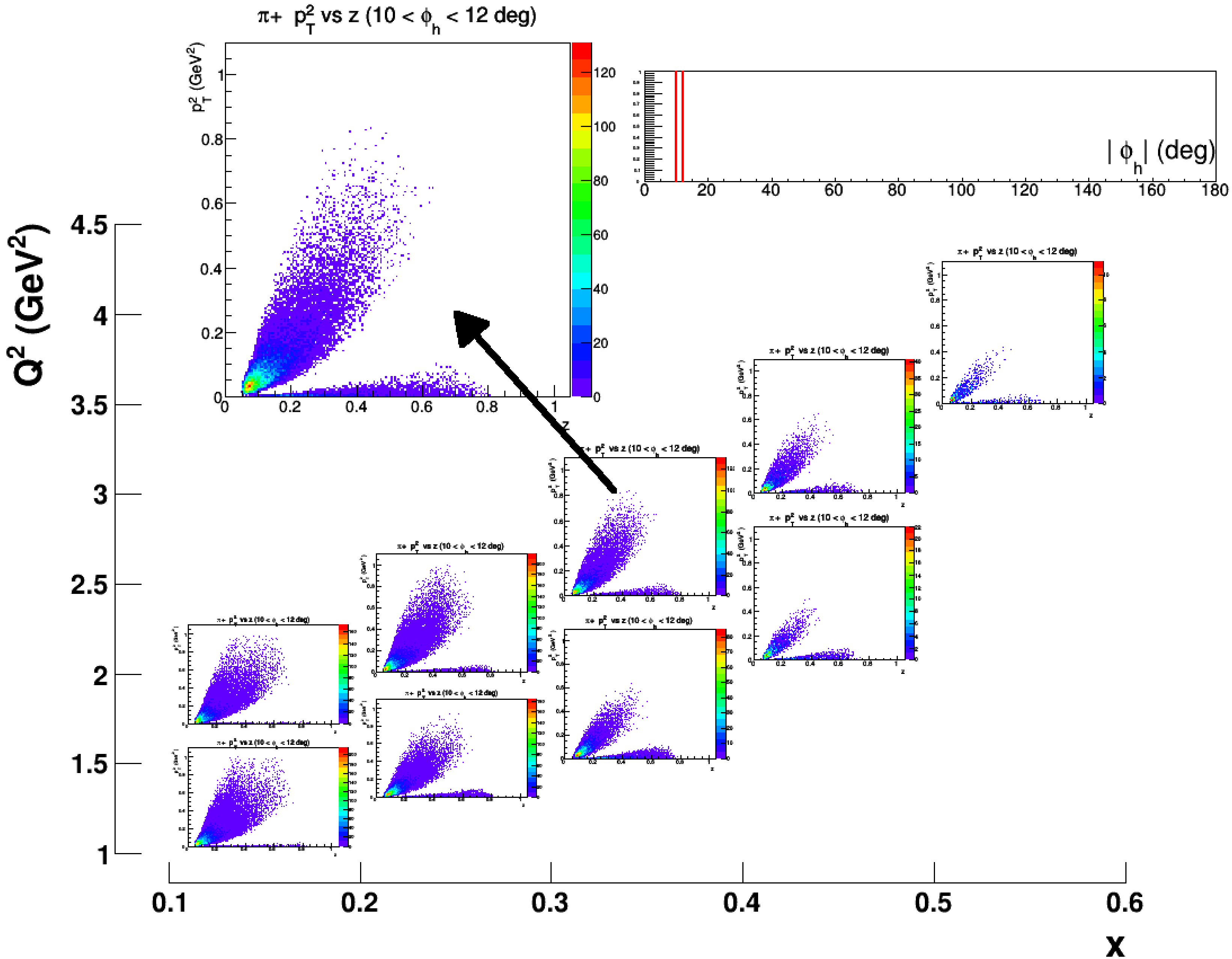

*Fully differential binning is necessary for understanding detector acceptance

animated plot: https://userweb.jlab.org/~nathanh/pip_5DaccPlot_scanPhih.gif

Radiative Corrections

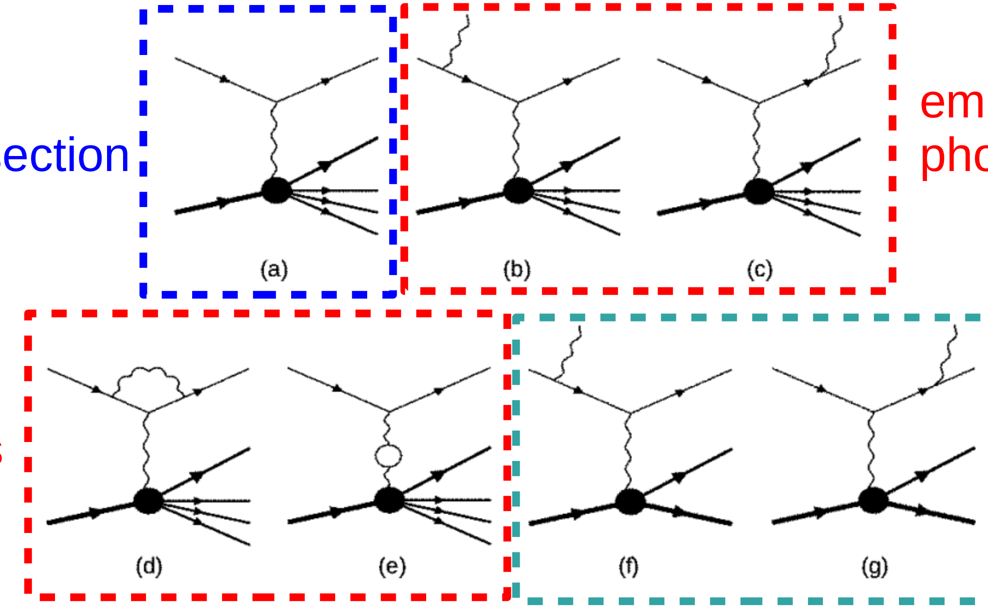

- Radiative effects, such as the emission of a photon by the incoming or outgoing electron, can change all five SIDIS kinematic variables.

- Furthermore, exclusive events can enter into the SIDIS sample because of radiative effects (“exclusive tail”).

- HAPRAD 2.0 is used to do radiative corrections.

- For a given $\sigma_{Born}\left(x, Q^2, z, P_{h\perp}^2, \phi_h\right)$ (obtained from a model), HAPRAD calculates $\sigma_{rad+tail}\left(x, Q^2, z, P_{h\perp}^2, \phi_h\right)$. The correction factor is then:

$$RC\ factor = \frac{\sigma_{rad+tail}\left(x, Q^2, z, P_{h\perp}^2, \phi_h\right)}{\sigma_{Born}\left(x, Q^2, z, P_{h\perp}^2, \phi_h\right)}$$

- 3 different models were used to study model dependence.

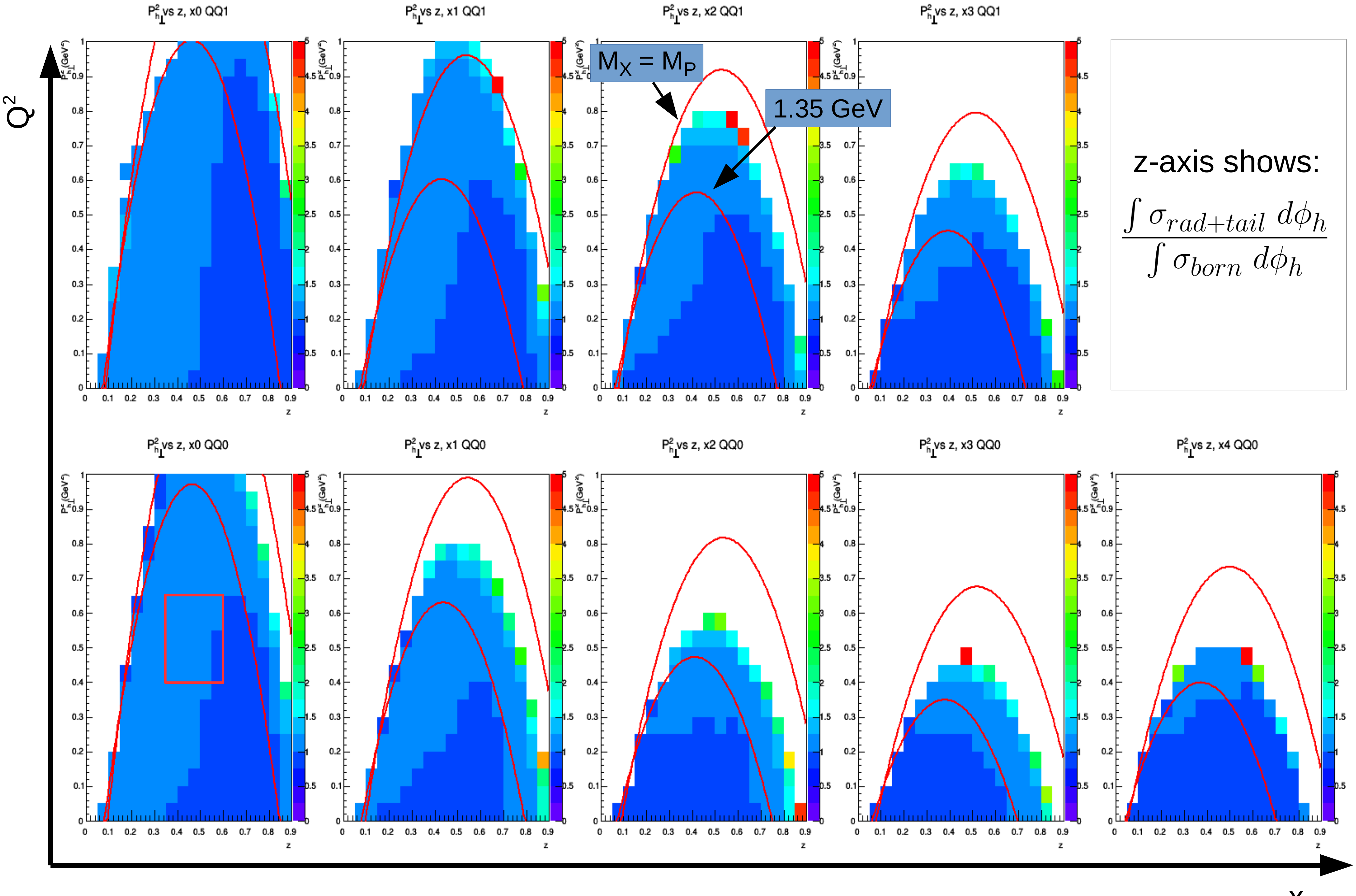

z-axis shows:

$$\frac{\int \sigma_{rad+tail}\, d\phi_h}{\int \sigma_{born}\, d\phi_h}$$

Born, radiated, and exclusive tail cross-sections from HAPRAD (lowest x-Q^2 bin)

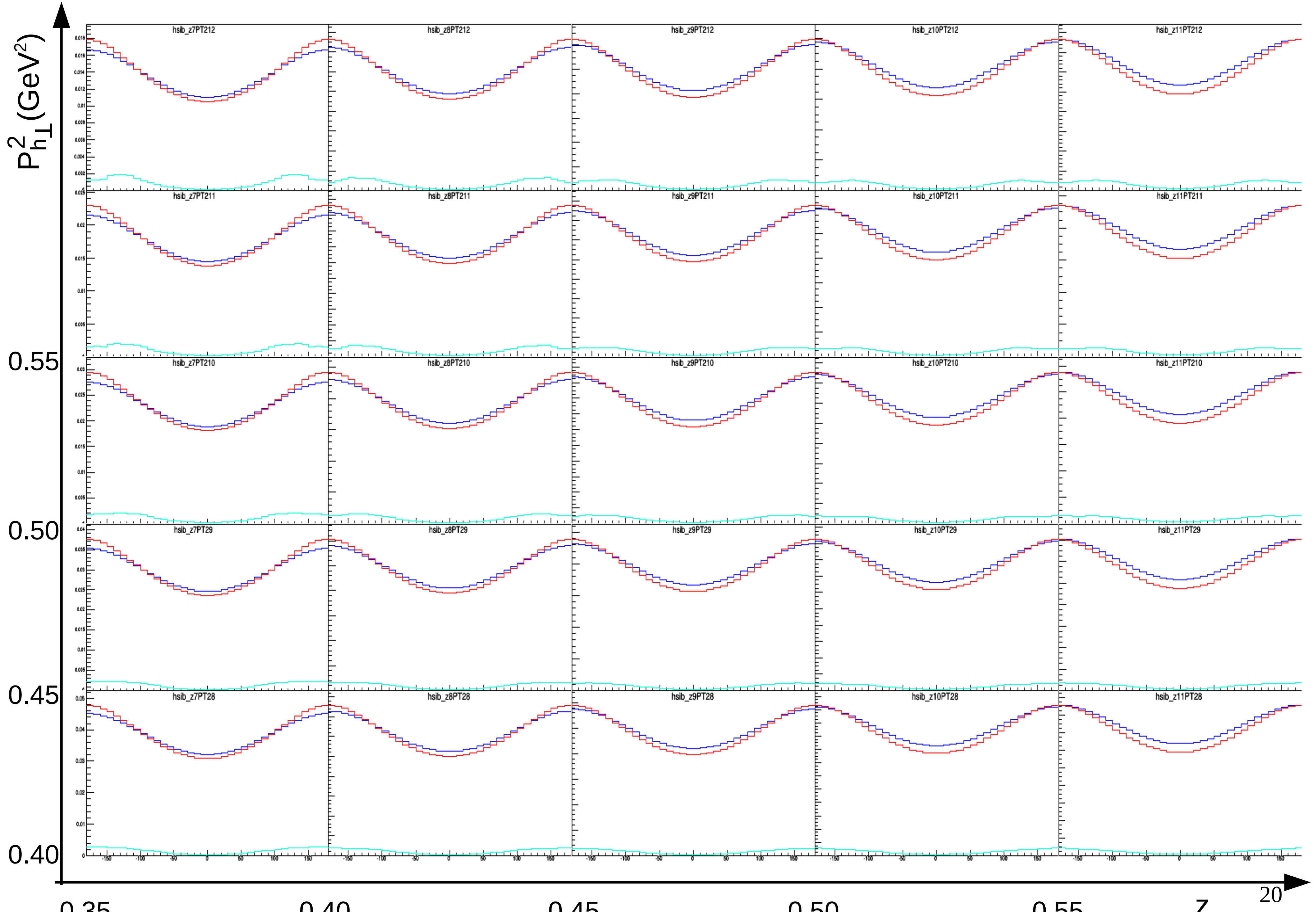

Born, radiated, and exclusive tail cross-sections from HAPRAD (lowest x-Q^2 bin)

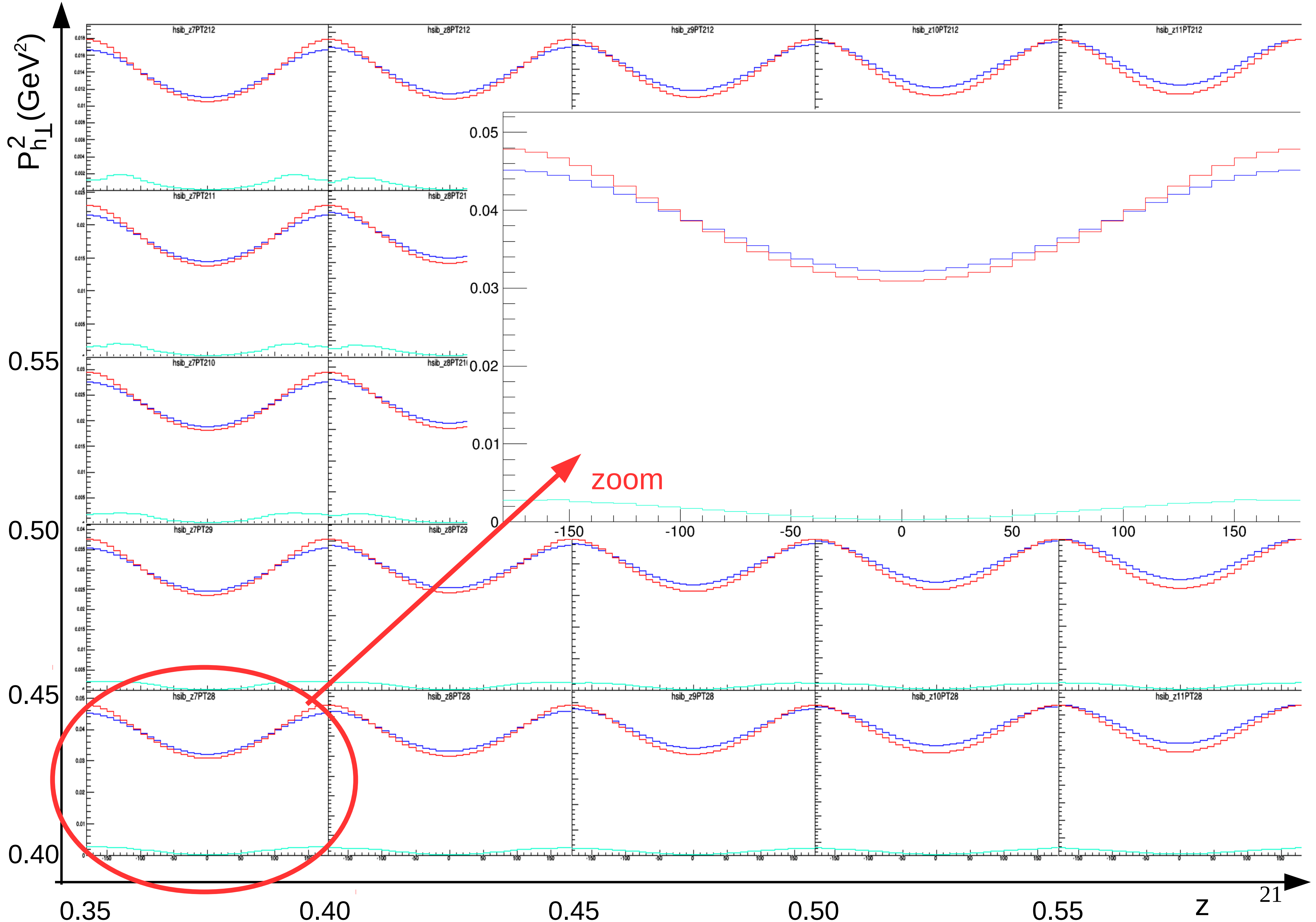

Final Results

φ_h distributions - raw data (lowest x-Q^2 bin)

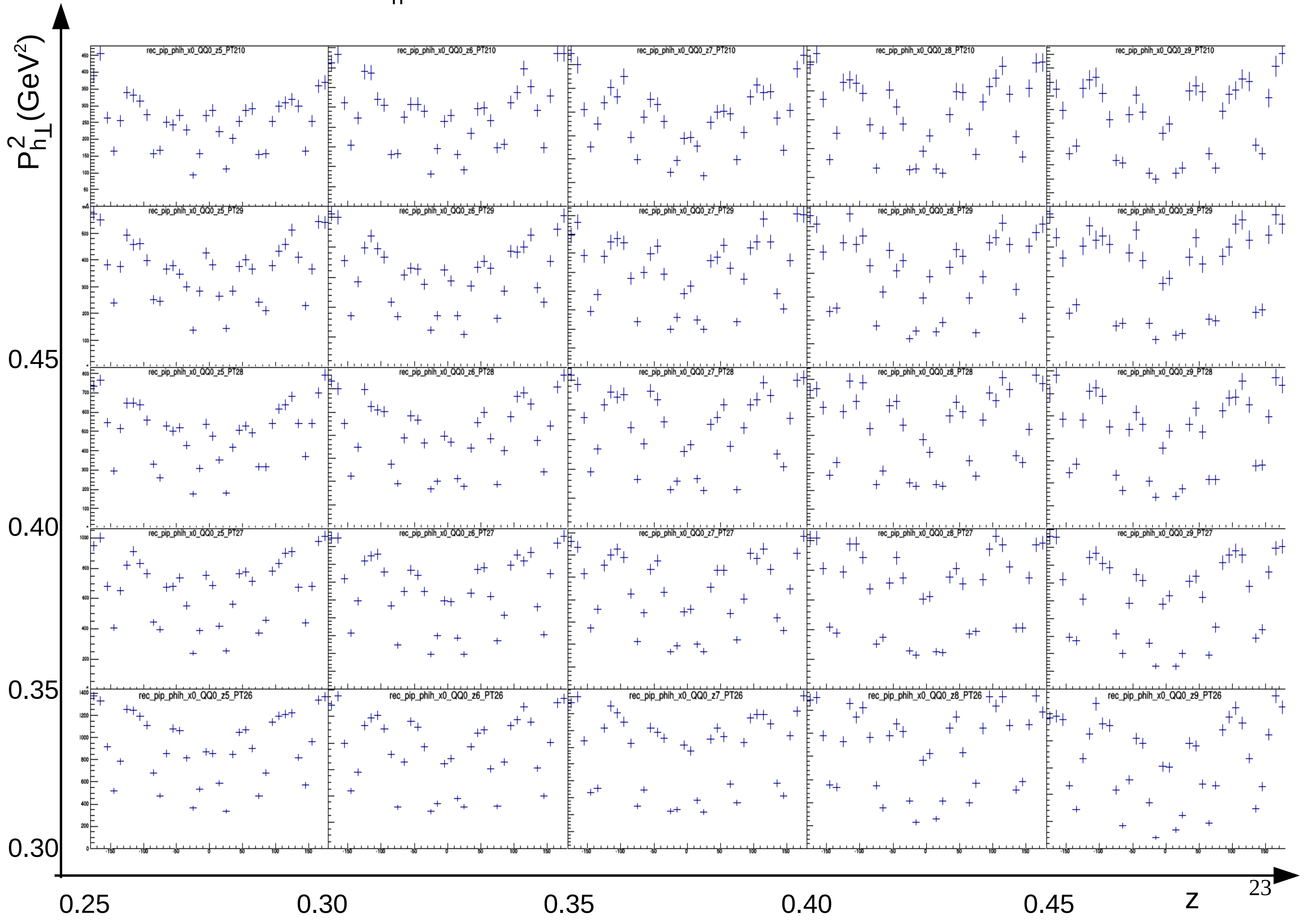

φ_h distributions – acceptance and radiative corrected with fit results (lowest x-Q^2 bin)

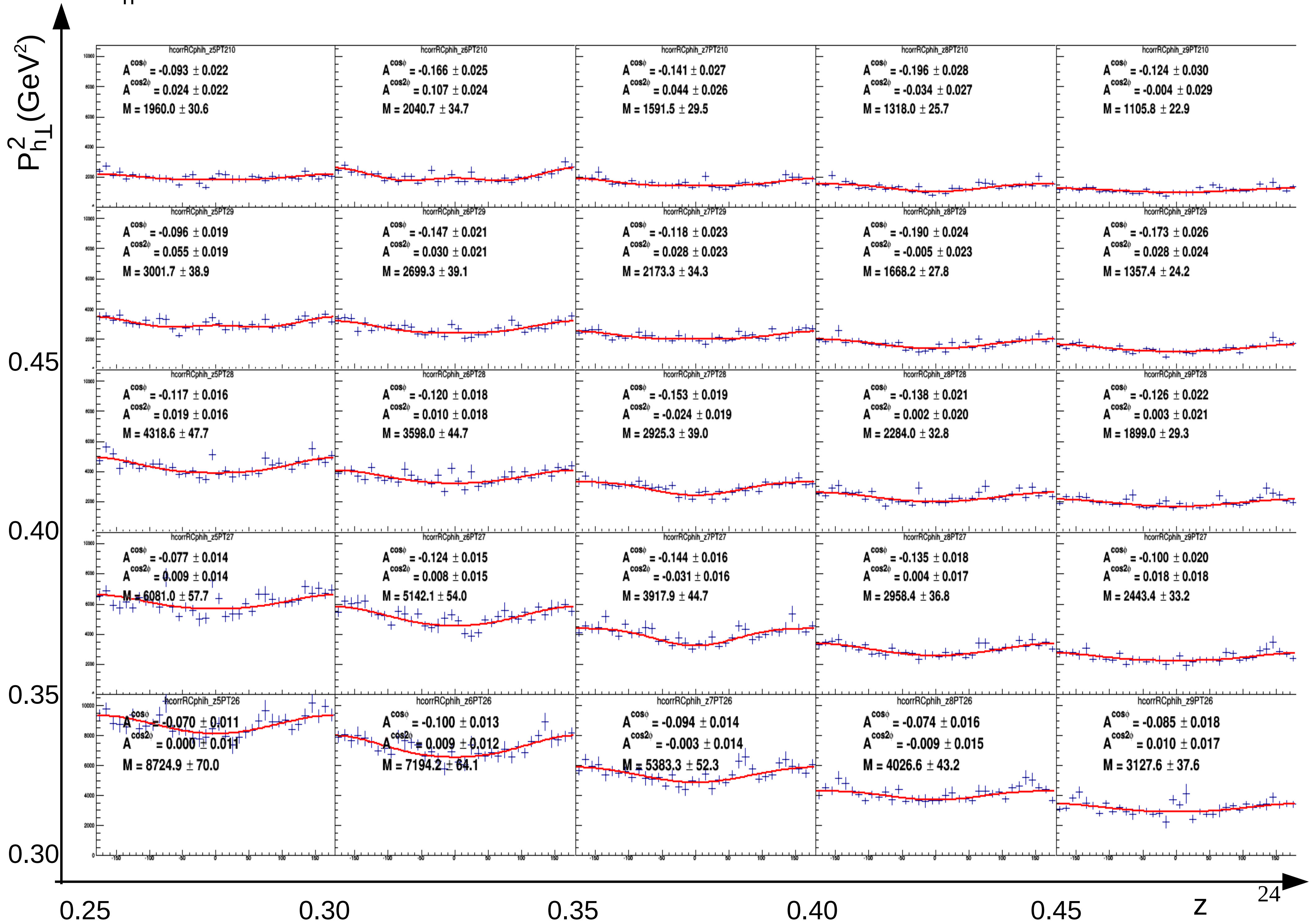

Representative Results

A_0 (top row), $A_{UU}^{\cos\phi_h}$ (middle row), and $A_{UU}^{\cos 2\phi_h}$ (bottom row) vs $P_{h\perp}^2$ for π+ and π-

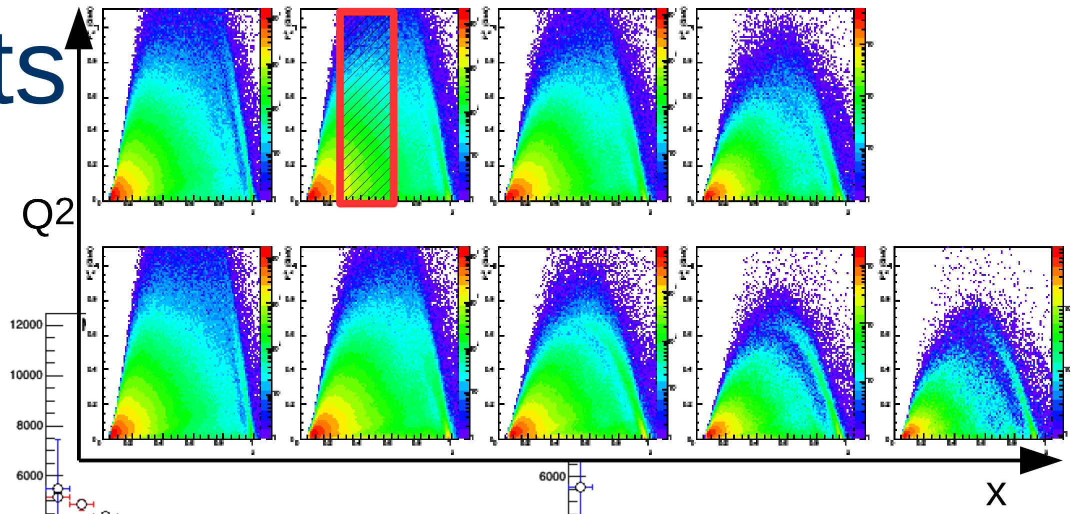

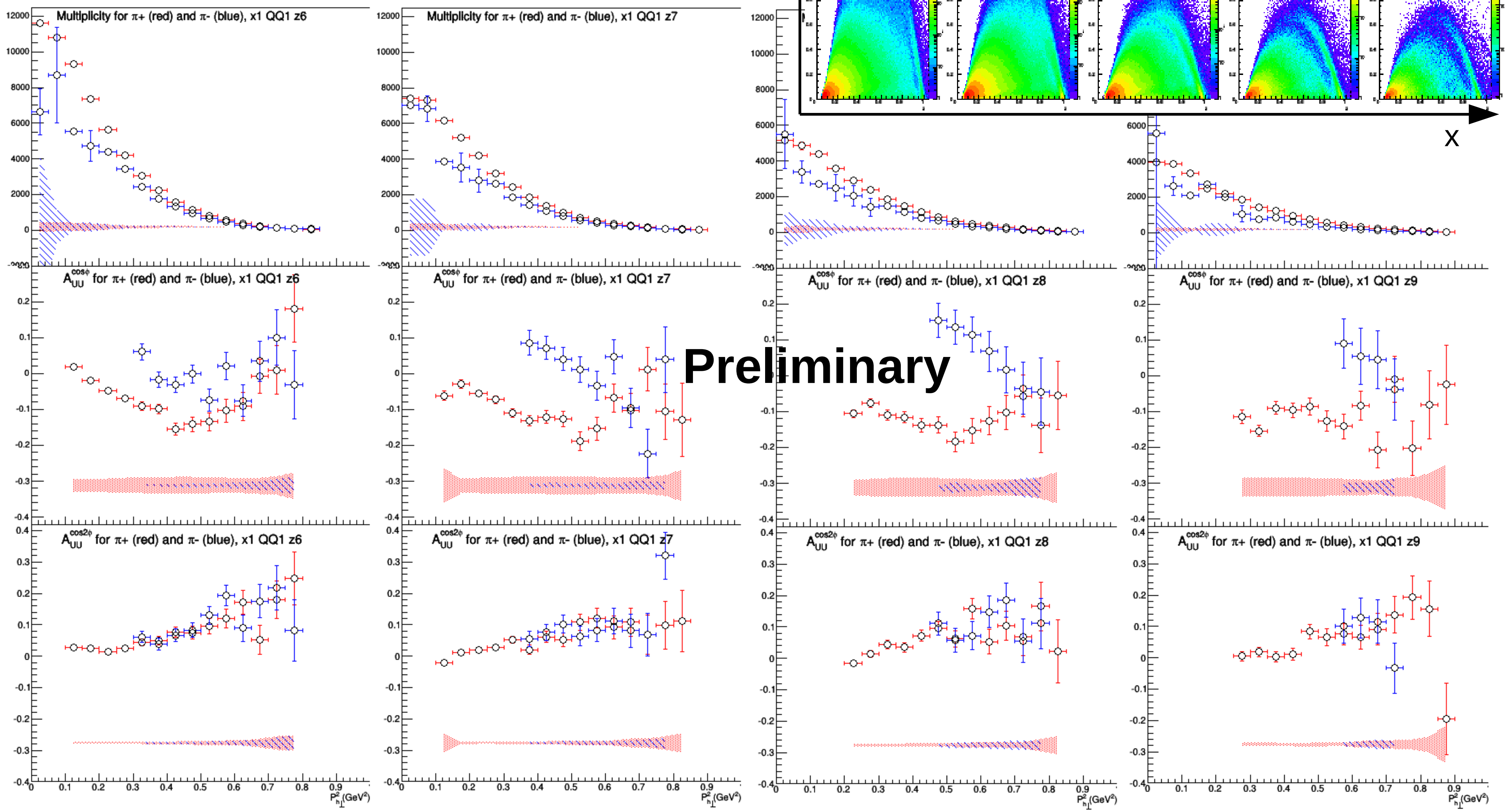

0.30 0.35 0.40 0.45 z

(high Q^2 bin of $0.2 < x < 0.3$)

Comparison with Other CLAS Data

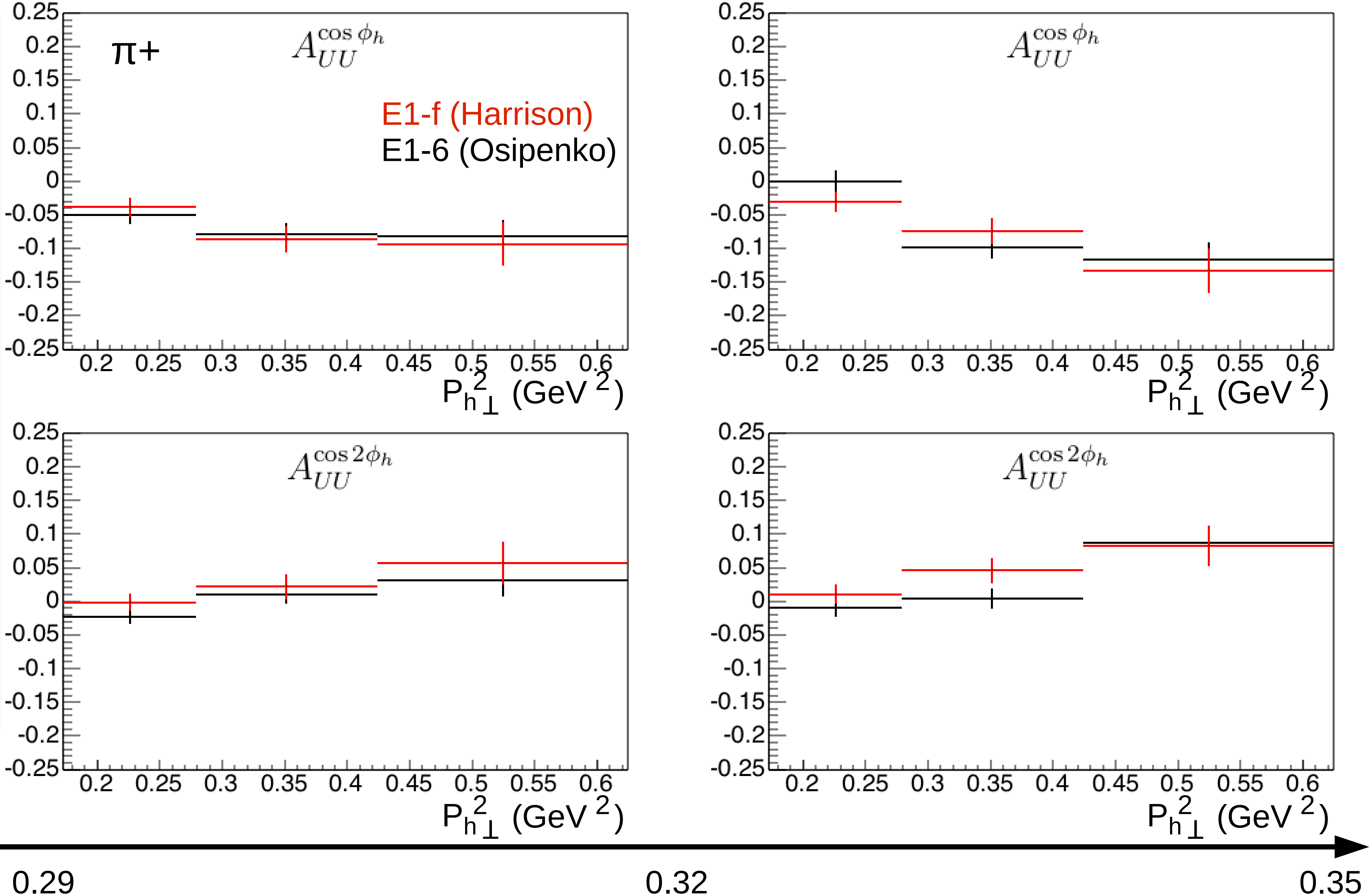

(0.25 < x < 0.28, 1.9 < Q^2 < 2.2 GeV^2)

z

Summary and Conclusions

- The multiplicity, $\cos\phi_h$ moment, and $\cos 2\phi_h$ moment of the unpolarized SIDIS cross-section have been measured for both charged pion channels in a fully differential way with good statistics and well controlled systematics over a wide kinematic range.

- The $\cos\phi_h$ and $\cos 2\phi_h$ modulations show a clear dependence on flavor which hints at a non-zero Boer-Mulders effect and could give insights into the quark orbital angular momentum contribution of the proton spin; but more intensive theoretical comparisons, which are currently in progress, are needed first.

- More thorough systematic error studies and comparisons are underway.

- Analysis note draft is complete and theoretical calculations have been promised by soon.

- A paper summarizing these results will be submitted soon to Phys.Rev.D.

Backup slides

TMDs

	twist-2 (leading twist)			twist-3 (sub-leading twist)
N\q	**U**	**L**	**T**	
U	f_1		$h_1^\perp$	$f^\perp, g^\perp, h, e$
L		g_{1L}	$h_{1L}^\perp$	$f_L^\perp, g_L^\perp, h_L, e_L$
T	$f_{1T}^\perp$	g_{1T}	$h_1, h_{1T}^\perp$	$f_T, f_T^\perp, g_T, g_T^\perp, h^\perp, e_T, h_T^\perp, e_T^\perp$

Boer-Mulders function

helicity function

worm gear functions

Sivers function

transversity function

pretzelosity or
Mulders-Tangerman function

- The formal definition of twist is twist = dimension – spin of the operator, however, twist = 2 + power of M/Q is often used for convenience.

- TMDs depend on the transverse momentum of the quark ($\mathbf{k}_T$) and on x, and describe un/longitudinally/transversely polarized quarks inside of un/longitudinally/transversely polarized nucleons.

- twist-2 TMDs describe a difference of probabilities for a particular quark to exist inside of a particular nucleon.

- twist-3 TMDs describe a quark-gluon correlation.

Interpretation of twist-2 TMDs:

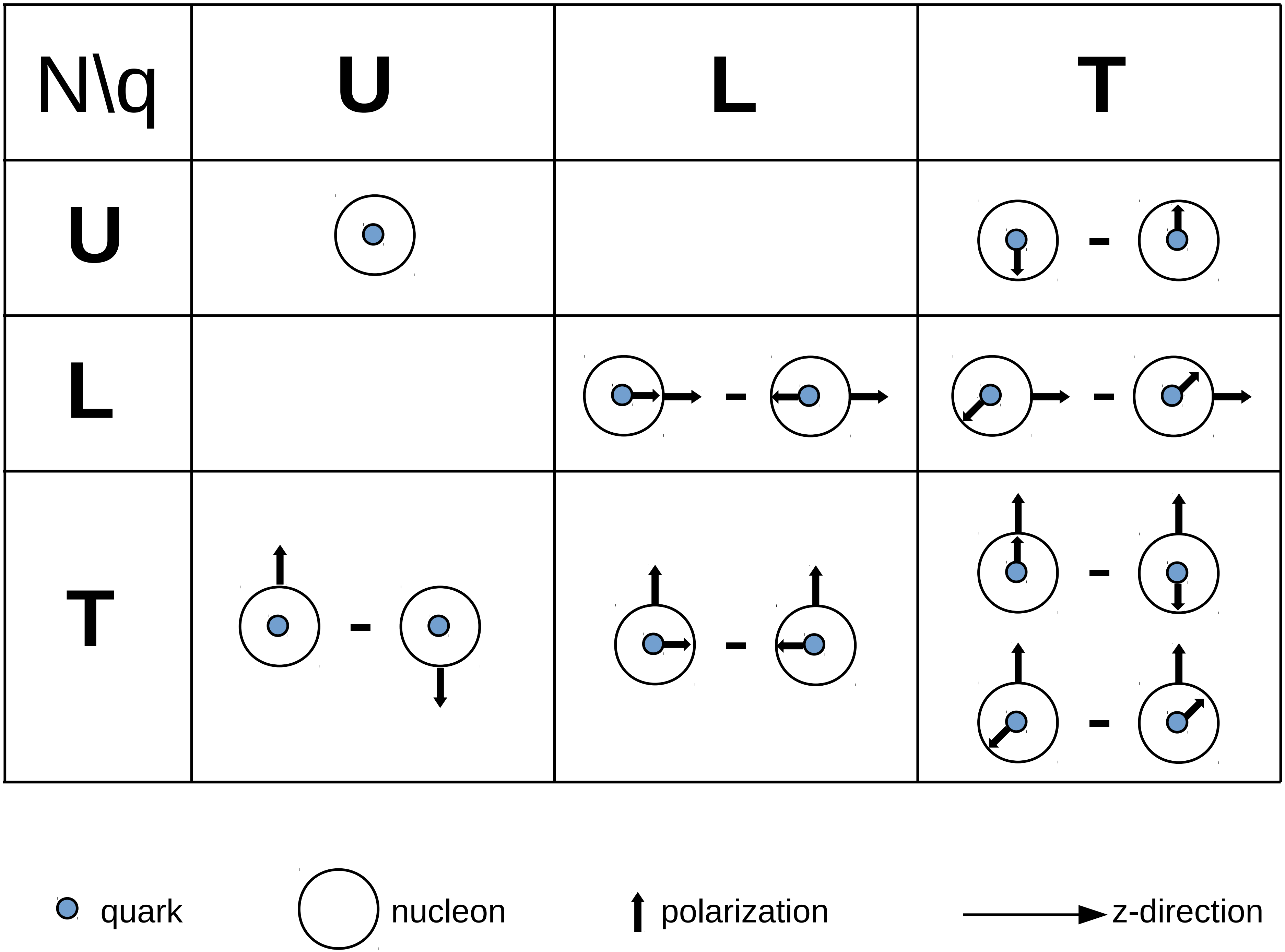

π^+ $P_{h\perp}^2$ vs z for each x-Q^2 bin

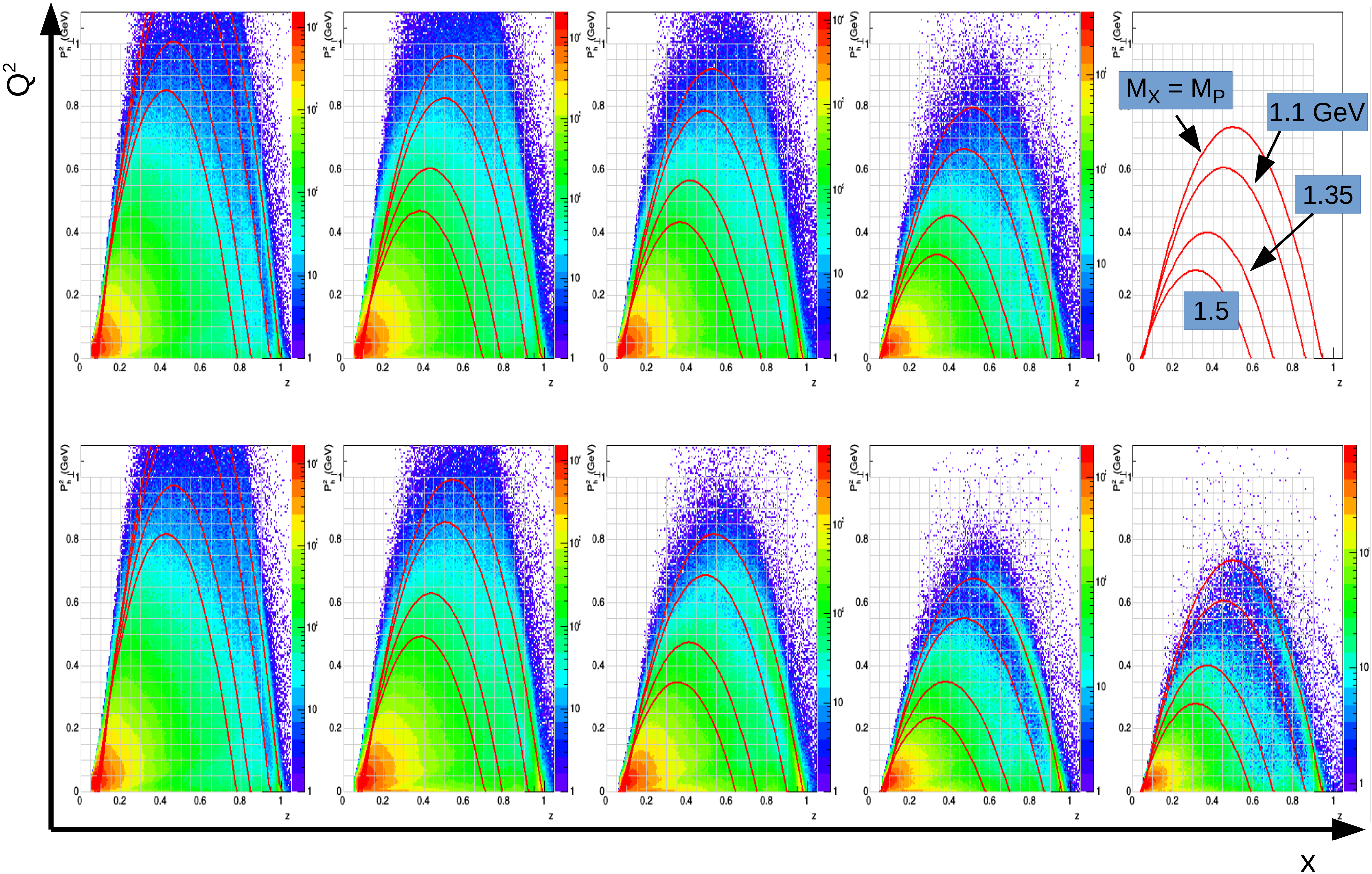

$\pi^- \ P_{h\perp}^2$ vs z for each x-Q^2 bin

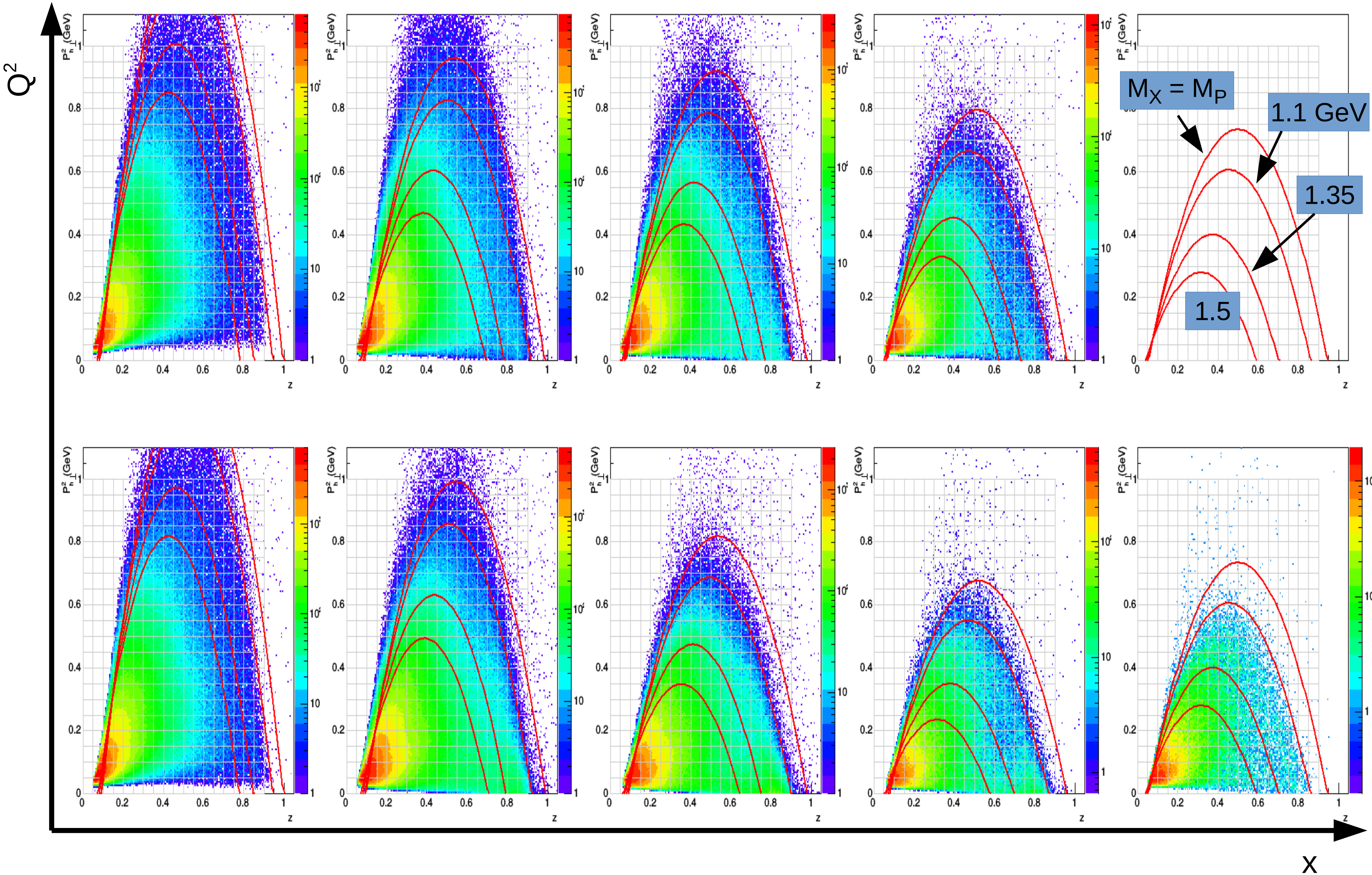

φ_h fiducial cuts

- $P_{h\perp}^2$ vs z plots on previous slides are integrated over φ_h.

- Animated plots show coverage in all 5 dimensions (x, Q^2, z, $P_{h\perp}^2$, φ_h).

  https://userweb.jlab.org/~nathanh/pip_data_zPT2fid_scanPhih.gif
  https://userweb.jlab.org/~nathanh/pim_data_zPT2fid_scanPhih.gif

- "Holes" in φ_h coverage create steep edges with unreliable reconstruction.

- Each x-Q^2-z-$P_{h\perp}^2$ bin has a φ_h cut (if necessary) to eliminate these regions, e.g.:

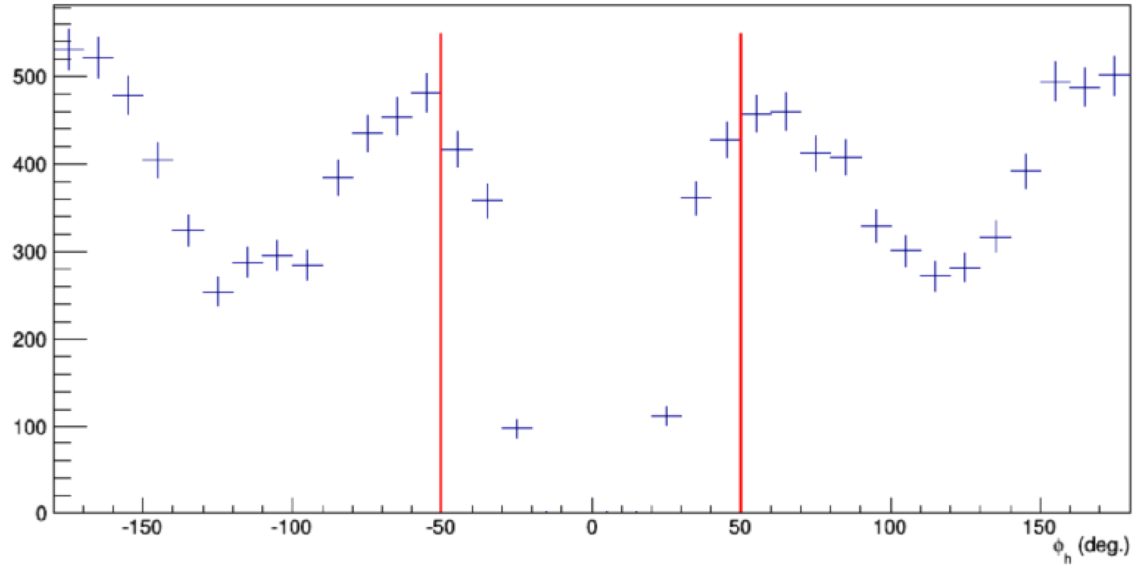

- Only multiplicity is extracted from bins with hole width > 60 degrees

Resolution Matching

- GSIM significantly overestimates the resolution in the CLAS detector; gpp was used to smear the MC to make it more realistic.

- Resolutions in the MC and data can be studied using the reaction:

$$ep \rightarrow e\pi^+\pi^-p$$

- Resolutions are defined as:

$$\Delta p = p_{calc} - p_{rec}$$

$$\Delta\theta = \theta_{calc} - \theta_{rec}$$

$$\Delta\phi = \phi_{calc} - \phi_{rec}$$

Δp in bins of $\theta_{\pi+}$ and $p_{\pi+}$

Data (black)

MC with DC smearing (red)

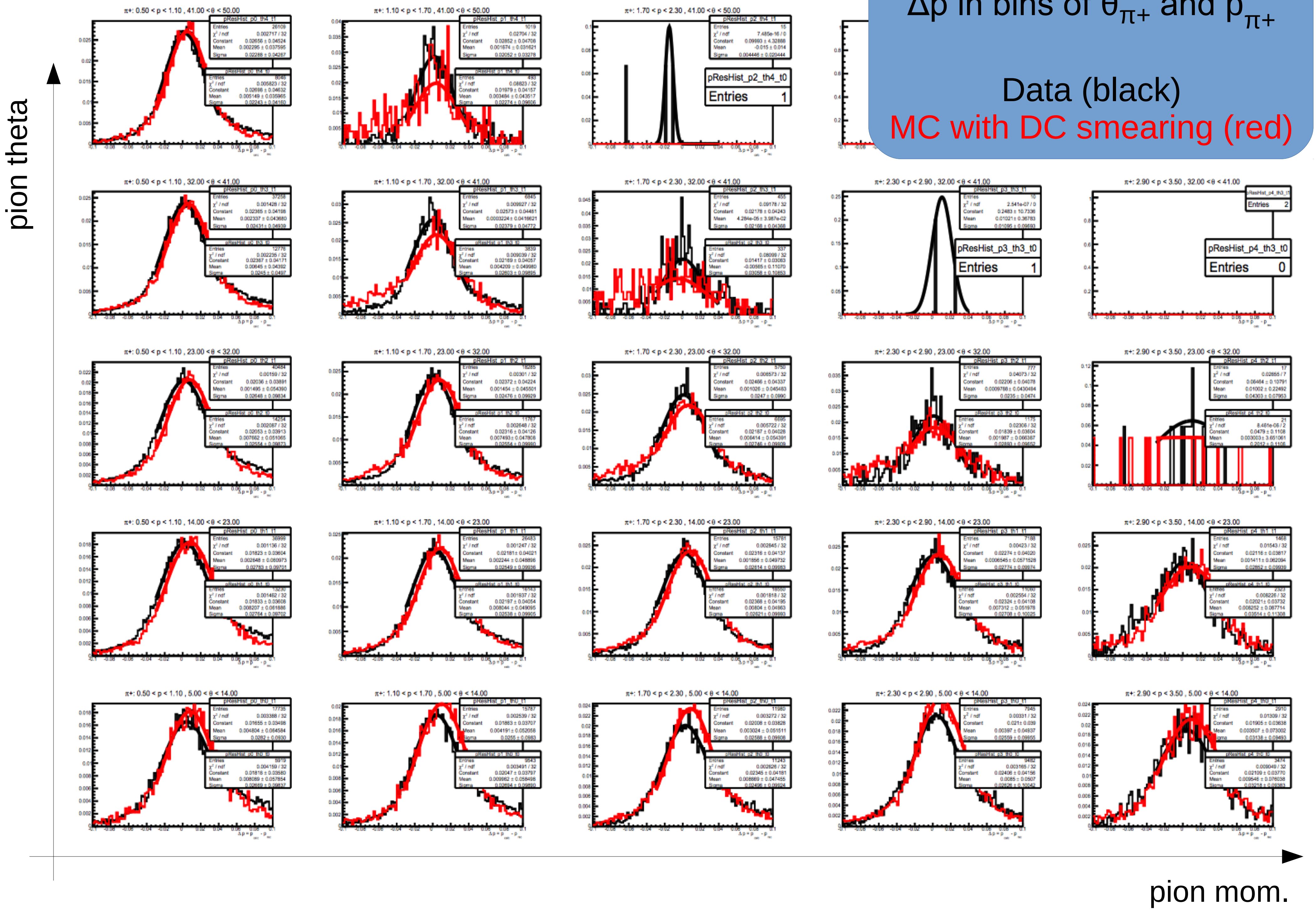

$\Delta\theta$ in bins of $\theta_{\pi+}$ and $p_{\pi+}$

Data (black)

MC with DC smearing (red)

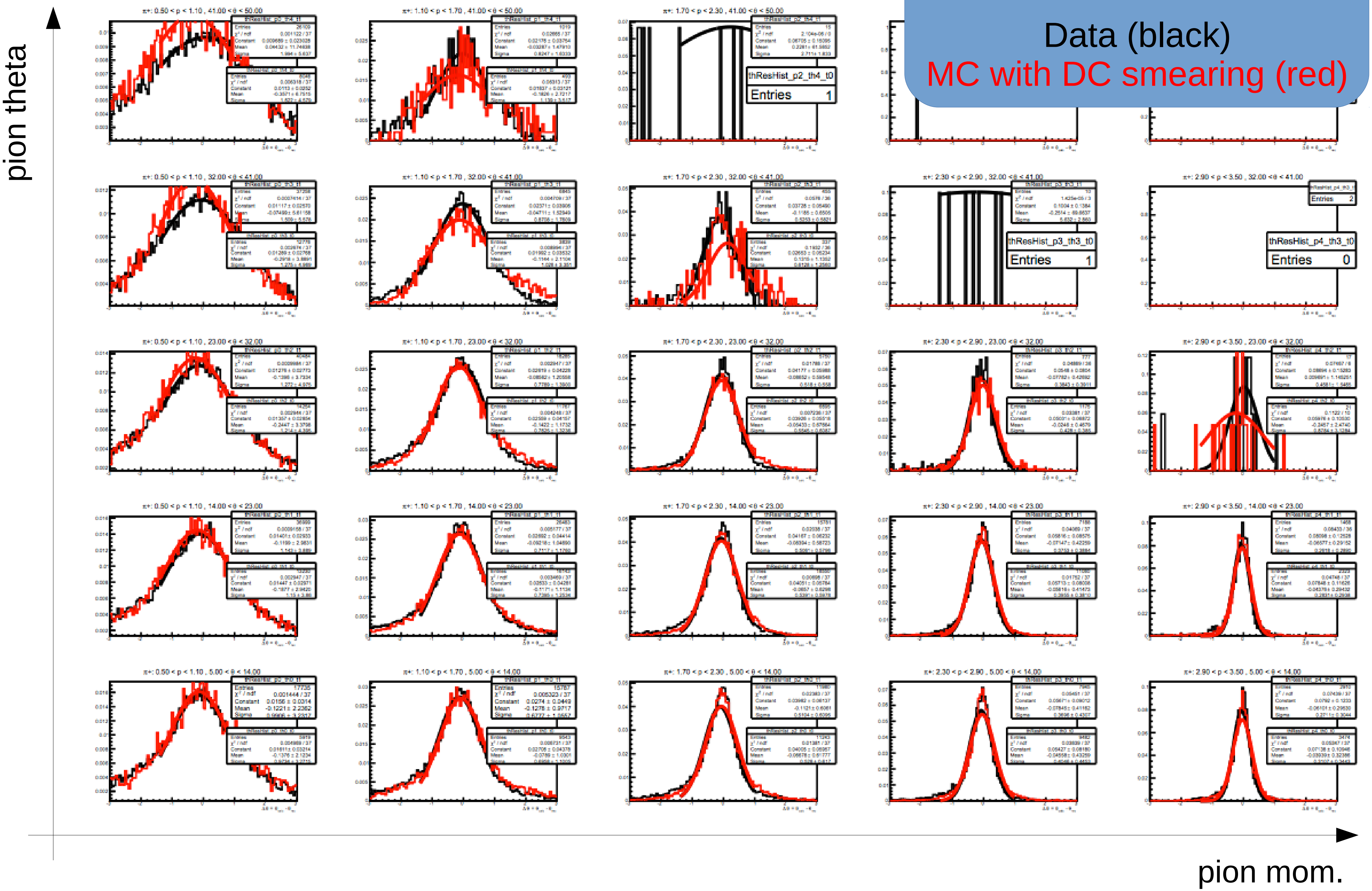

$\Delta\varphi$ in bins of $\theta_{\pi+}$ and $p_{\pi+}$

Data (black)
MC with DC smearing (red)

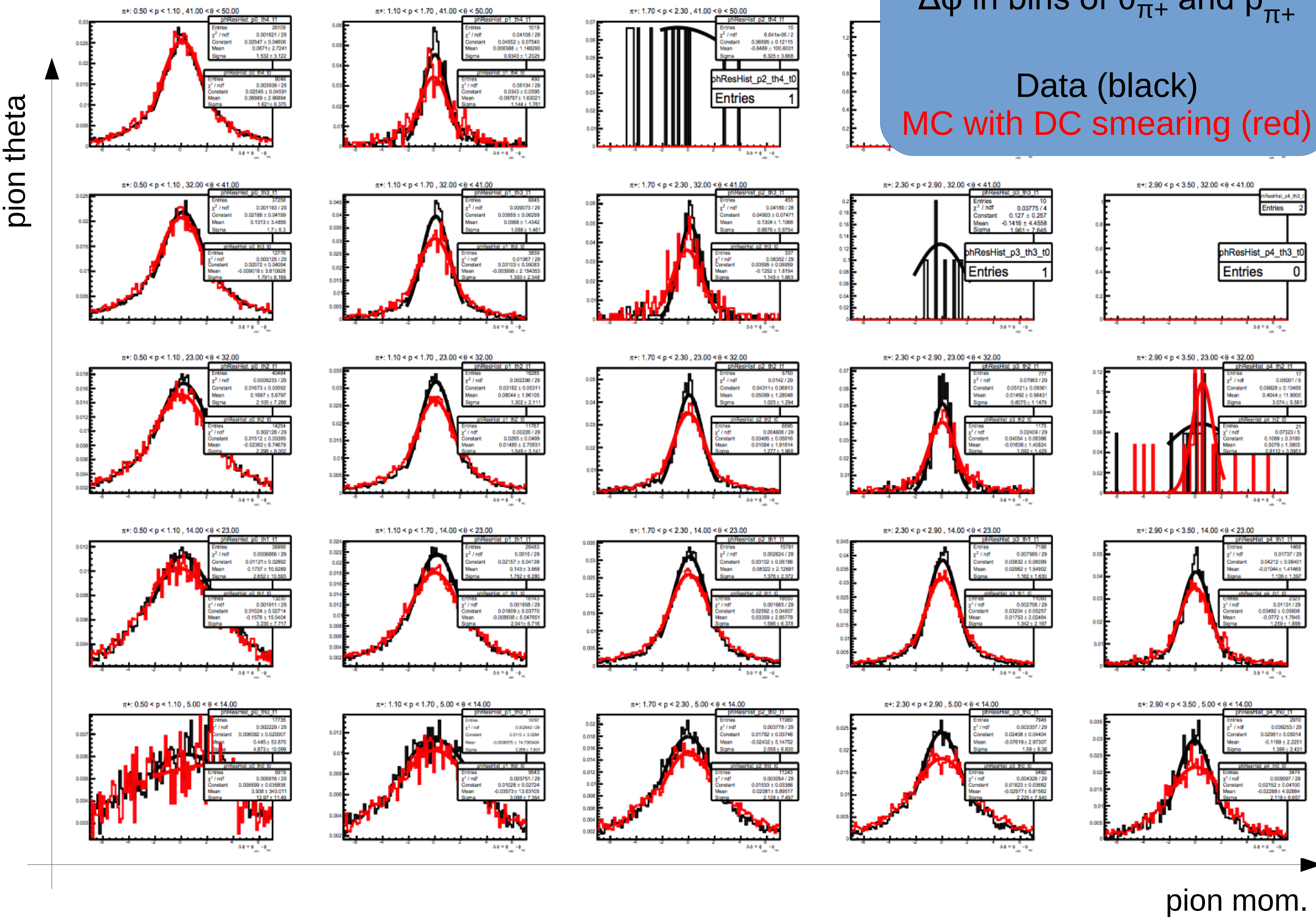

π^+ β in momentum bins

Data (black)

MC with TOF smearing (red)

Low momentum

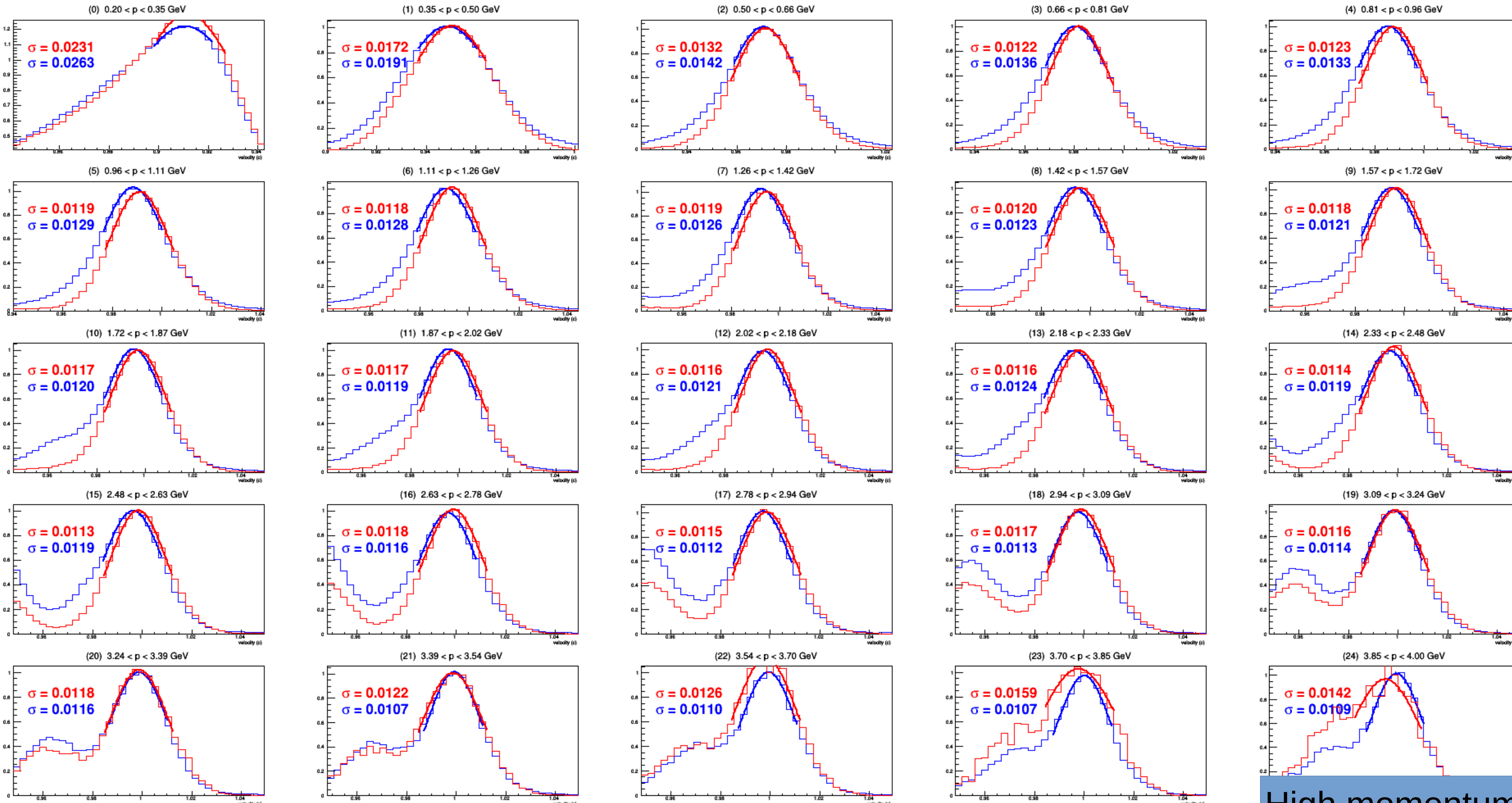

High momentum

Effects of the shape of the generated ϕ distribution

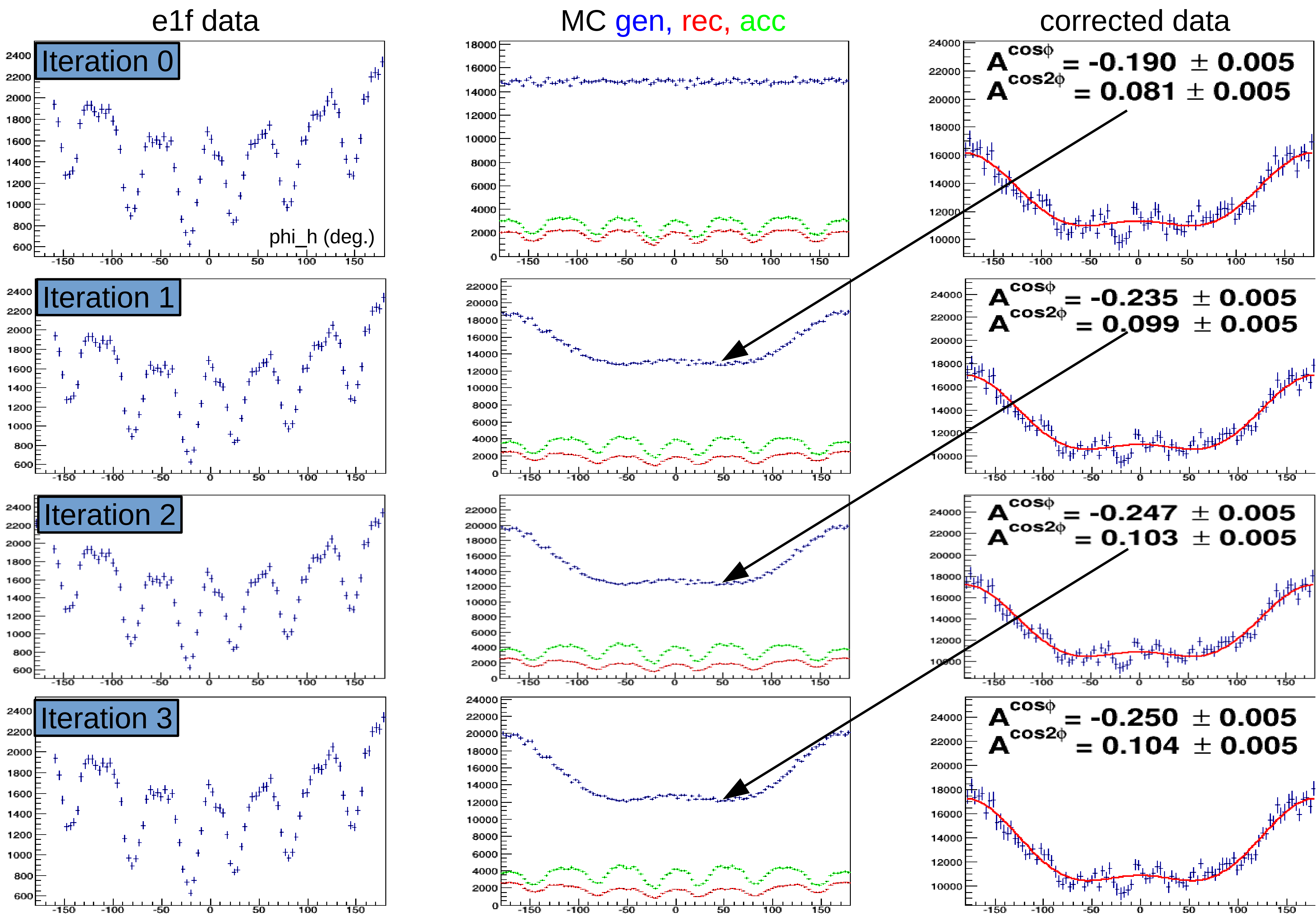

Systematic Errors

- 13 sources of systematic error are tested:

Label	Source	N variations
0	e- z-vertex cut	2
1	e- EC sampling cut	2
2	e- EC outer vs inner cut	2
3	e- EC geometric cut	2
4	e- CC θ matching cut	2
5	e- region 1 fiducial cut	2
6	e- region 3 fiducial cut	2
7	e- CC fiducial cut	2
8	pion β cut	2
9	pion region 1 fiducial cut	2
10	φ_h fiducial cut	2
11	acceptance model dependence	1
12	RC model dependence	1

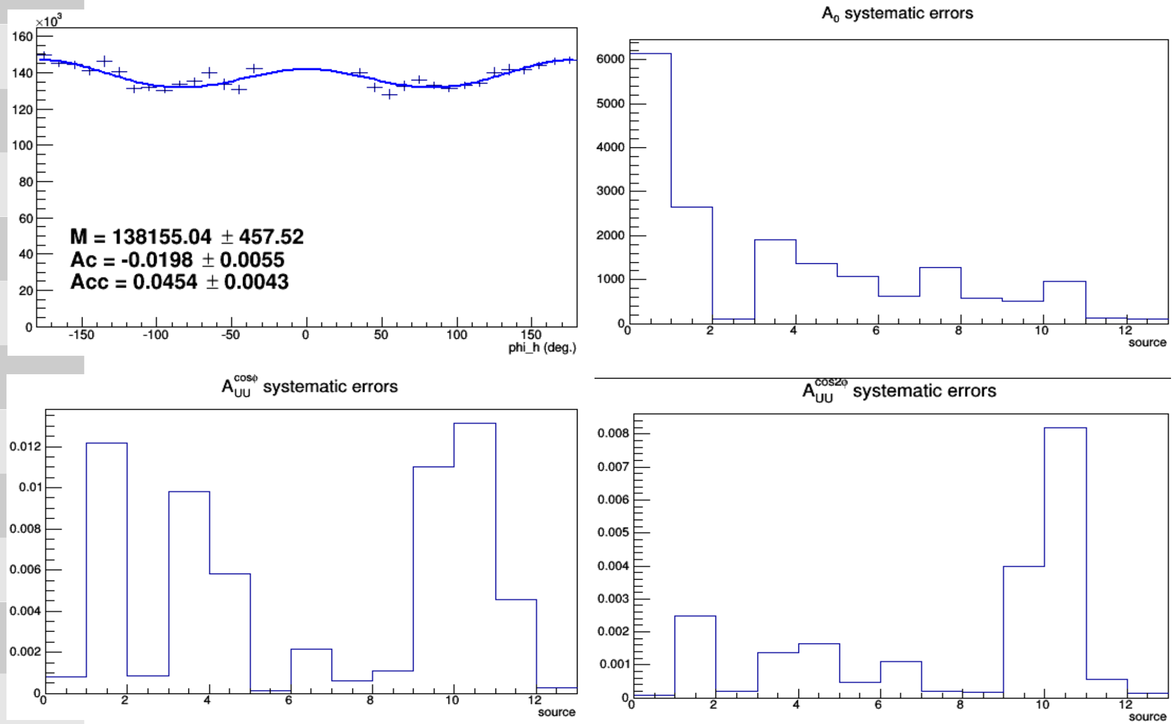

Above: systematic error results for a representative bin. (π+ bin 0 0 3 0)

- Error from source i is given by:

$$\Delta^i_{RMS} = \frac{\sqrt{\sum_j^{N_v^i} \Delta_j^2}}{\sqrt{N_v^i}}$$

- The contributions from each source are added in quadrature.